ผลของโลหะทรานซิชันที่เติมบนตัวเร่งปฏิกิริยาวาเนเดียมฟอสฟอรัสออกไซด์ ในปฏิกิริยาออกซิเดชันบางส่วนของนอร์มอล-เพนเทน

นางสาวสุชานุช พิศุทธางกูร

วิทยานิพนธ์นี้เป็นส่วนหนึ่งของการศึกษาตามหลักสูตรปริญญาวิศวกรรมศาสตรมหาบัณฑิต
สาขาวิชาวิศวกรรมเคมี ภาควิชาวิศวกรรมเคมี
คณะวิศวกรรมศาสตร์ จุฬาลงกรณ์มหาวิทยาลัย
ปีการศึกษา 2559

EFFECT OF TRANSITION METALS PROMOTED ON VANADIUM PHOSPHORUS OXIDE (VPO) CATALYSTS IN THE PARTIAL OXIDATION OF N-PENTANE

Miss Suchanut Pisuttangkul

A Thesis Submitted in Partial Fulfillment of the Requirements
for the Degree of Master of Engineering Program in Chemical Engineering
Department of Chemical Engineering
Faculty of Engineering
Chulalongkorn University
Academic Year 2016

Thesis Title	EFFECT OF TRANSITION METALS PROMOTED ON VANADIUM PHOSPHORUS OXIDE(VPO) CATALYSTS IN THE PARTIAL OXIDATION OF N-PENTANE
By	Miss Suchanut Pisuttangkul
Field of Study	Chemical Engineering
Thesis Advisor	Associate Professor Joongjai Panpranot, Ph.D.

Accepted by the Faculty of Engineering, Chulalongkorn University in Partial Fulfillment of the Requirements for the Master's Degree

.....Dean of the Faculty of Engineering

(Associate Professor Supot Teachavorasinskun, D.Eng.)

THESIS COMMITTEE

.....Chairman

(Professor Bunjerd Jongsomjit, Ph.D.)

.....Thesis Advisor

(Associate Professor Joongjai Panpranot, Ph.D.)

.....Examiner

(Chutimon Satirapipathkul, D.Eng.)

.....External Examiner

(Assistant Professor Okorn Mekasuwandumrong, D.Eng.)

.....External Examiner

(Associate Professor Tawan Sooknoi, Ph.D.)

สุชานุช พิศุทธางกูร : ผลของโลหะทรานซิชันที่เติมบนตัวเร่งปฏิกิริยาวาเนเดียมฟอสฟอรัสออกไซด์ ในปฏิกิริยาออกซิเดชันบางส่วนของนอร์มอล-เพนเทน (EFFECT OF TRANSITION METALS PROMOTED ON VANADIUM PHOSPHORUS OXIDE(VPO) CATALYSTS IN THE PARTIAL OXIDATION OF N-PENTANE) อ.ที่ปรึกษาวิทยานิพนธ์หลัก: จูงใจ ปั้นประณต, 62 หน้า.

วาเนเดียมฟอสฟอรัสออกไซด์เป็นตัวเร่งปฏิกิริยาที่ใช้ในปฏิกิริยาออกซิเดชันบางส่วนของนอร์มอล-บิวเทนและนอร์มอลเพนเทน ในงานวิจัยนี้เตรียมตัวเร่งปฏิกิริยาวาเนเดียมฟอสฟอรัสออกไซด์โดยการรีฟลักซ์วาเนดิลฟอสเฟตไดไฮเดรตกับไอโซบิวทานอล และทำการดัดแปรตัวเร่งปฏิกิริยา โดยการเติมตัวส่งเสริมโลหะทรานซิชันนั่นได้แก่ โคบอลต์ บิสมัท เหล็ก และ แมงกานีส โดยในส่วนแรกใช้อัตราส่วนโดยมวลของโลหะตัวส่งเสริมต่อวาเนเดียมเท่ากับ 0.35 พบว่าตัวส่งเสริมแมงกานีสเพิ่มประสิทธิภาพของตัวเร่งปฏิกิริยา ในปฏิกิริยาออกซิเดชันบางส่วนของนอร์มอลเพนเทนได้ดีที่สุด จากนั้นศึกษาการเติมตัวส่งเสริมแมงกานีสในปริมาณที่ต่างกัน ที่อัตราส่วนโดยมวลของแมงกานีสต่อวาเนเดียมเท่ากับ 0.25 0.38 0.45 0.55 และ 0.65 ตัวเร่งปฏิกิริยาทั้งหมดที่เตรียมผ่านการเผาที่อุณหภูมิ 300 องศาเซลเซียส เป็นเวลา 8 ชั่วโมง เพื่อผลิตเฟสของวาเนดิล ไพโรฟอสเฟต ซึ่งเป็นเฟสที่ว่องไวของตัวเร่งปฏิกิริยา ซึ่งสามารถยืนยันได้จากการวิเคราะห์ด้วยเทคนิคการเลี้ยวเบนของรังสีเอกซ์ ผลจากกล้องจุลทรรศน์อิเล็กตรอนแบบส่องกราดแสดงสัณฐานของตัวเร่งปฏิกิริยาที่มีลักษณะแบบกลีบกุหลาบของวาเนดิลไพโรฟอสเฟต นอกจากนี้พบว่าการเติมตัวส่งเสริมโลหะทรานซิชันส่งผลให้เกิดออกซิเดชันของวาเนเดียมสี่บวกมากขึ้น ซึ่งช่วยทำให้ตัวเร่งปฏิกิริยามีประสิทธิภาพที่ดีขึ้น โดยค่าการเปลี่ยนแปลงนอร์มอล-เพนเทนของตัวเร่งปฏิกิริยาอยู่ในช่วง 42.7-55.8 เปอร์เซ็นต์ ค่าการเลือกเกิดมาเลอิกแอนไฮไดร์ 28.9-62.5 เปอร์เซ็นต์ และฟาทาลิกแอนไฮไดร์ 8-13.1 เปอร์เซ็นต์ อัตราส่วนของแมงกานีสต่อวาเนเดียมที่ทำให้ตัวเร่งปฏิกิริยามีประสิทธิภาพสูงที่สุดคือ 0.45

ภาควิชา วิศวกรรมเคมี ลายมือชื่อนิสิต .....

สาขาวิชา วิศวกรรมเคมี ลายมือชื่อ อ.ที่ปรึกษาหลัก .....

ปีการศึกษา 2559

5870256021 : MAJOR CHEMICAL ENGINEERING

KEYWORDS: MALEIC ANHYDRIDE (MA) / PHTHALIC ANHYDRIDE(PA) / VANADIUM PHOSPHORUS OXIDE (VPO) CATALYST / TRANSITION METAL DOPANTS / PARTIAL OXIDATION OF N-PENTANE

SUCHANUT PISUTTANGKUL: EFFECT OF TRANSITION METALS PROMOTED ON VANADIUM PHOSPHORUS OXIDE(VPO) CATALYSTS IN THE PARTIAL OXIDATION OF N-PENTANE. ADVISOR: ASSOC. PROF. JOONGJAI PANPRANOT, Ph.D., 62 pp.

Vanadium phosphorus oxide (VPO) catalysts have been employed in partial oxidation of n-butane and n-pentane. In this study, VPO catalysts were synthesized by refluxing vanadyl phosphate dihydrate ($VOPO_4 \bullet 2H_2O$) with isobutanol and modified with transition metals promoters such as Co, Bi, Fe, and Mn at the mass ratio of M/V 0.35. In the first part, Mn was found to be the best metal to improve the performances of VPO catalyst in n-pentane oxidation. Then the Mn-VPO catalysts were prepared with different ratios of Mn/V loadings at 0.25, 0.35, 0.45, 0.55, and 0.65. All the catalysts were calcined at 300^{o}C for 8 h to generate the vanadyl pyrophosphate ($(VO)_2P_2O_7$) phase which is the active phase of VPO catalysts and was confirmed by the XRD results. As shown by SEM results, all the synthesized catalysts showed the rosette-shape morphologies of vanadyl pyrophosphate. The transition metal promoted catalysts presented the formation of V^{4+} state which provided a better catalytic performance with 42.7-55.8% n-pentane conversion, 28.9-62.5% MA selectivity, and 8-13.1% PA selectivity. The optimum ratio of Mn/V was determined to be at 0.45

Department: Chemical Engineering Student's Signature .....

Field of Study: Chemical Engineering Advisor's Signature .....

Academic Year: 2016

ACKNOWLEDGEMENTS

The work described in this research could not have been completed without the assistance of many people. First, a very special thank you to my thesis advisor, Assoc. Prof. Dr. Joongjai Panpranot for her invaluable help and her great explain to clearly things. Throughout my thesis writing period, she provided encouragement, good teaching, and give lots of ideas to me.

I would like to express my sincere appreciation to Prof. Dr. Piyasan Praserthdam for his supervision and any advices throughout this research. In addition, I would like to thank the officer and scientists at the center of excellence on catalysis and catalytic reaction engineering, Department of chemical engineering, Faculty of engineering, Chulalongkorn University for their help and carried out the catalytic analyses.

Finally, I would like to thank my family and friends for their support, conviction and consolation throughout the period of this work.

CONTENTS

Page

Page

Page

LIST OF FIGURES

LIST OF TABLES

CHAPTER 1
INTRODUCTION

1.1 General introduction

Maleic anhydride (MA) and phthalic anhydride (PA) are used in the production of unsaturated polyester resins (UPR) [1], the manufacture of plastics, fibers, lacquers, and paints, etc. In chemical industry, MA and PA are the main intermediates. MA is produced by the selective of hydrocarbons that is benzene and butane. In 1930, MA was produced by the selective oxidation of benzene due to low cost and medium – size plants. But now, the cost of benzene is very high so butane based process is preferred route used by most manufacturers [2]. PA was discovered in 1836 by Auguste Laurent [3] . It was produced by oxidation of o-xylene, naphthalene, and pentane. n-pentane is the reactant that can produce both MA and PA. In this research, it is interested in both of MA and PA production by the partial oxidation of n-pentane.

Transforming of low value hydrocarbons into the valuable industrial products remain as the best incentive for research. Normal pentane is a hydrocarbon that has many advantages such as less expensive, relative safety, and low boiling point, etc. Vanadium phosphorus oxides (VPO) are important catalyst. They are used for the partial oxidation of n-pentane to MA and PA. Main byproducts from this reaction are also carbon monoxide (CO) and carbon dioxide (CO_2).

Vanadium phosphorus oxides (VPO) were prepared using the precipitation method. The established vanadyl pyrophosphate ($(VO)_2P_2O_7$) behaves as a substrate for the other VPO phases such as α-, β-, and γ-$VOPO_4$. 3 phase of $(VO)_2P_2O_7$ are important for n-pentane oxidation processes [4],[5]. $(VO)_2P_2O_7$ is the active phase of catalyst and this phase is prepared by calcination of vanadium phosphate hemihydrate ($VOPO_4 \bullet 0.5H_2O$). The main strategy for synthesis of catalysts is a mixture of vanadium (IV) oxide (V_2O_5) and ortho-phosphoric acid (H_3PO_4) with an alcohol. Some researchers reported that V^{5+} and V^{4+} species present the topmost oxidation state of vanadyl pyrophosphate and that oxidation state are responsible for catalyst activity [5]. So anyway, both of oxidation state and phase composition of VPO catalyst are highly dependent on the preparation of catalyst precursor but it was not sufficient for improving the product selectivity. An attempt has been made to increase selective of MA and PA by adding the second metal promoter. Furthermore, from Cabani, F. et al. (1997) [6] investigation, the modification of metal dopping on VPO catalyst considered

to have higher activity for the selective oxidation of n-pentane reaction and higher products selectivity when compared to VPO undoped catalyst.

In this research, the transition metals used as the second metal promoter are bismuth (Bi), cobalt (Co), iron (Fe), and manganese (Mn). The catalysts were characterized by X-ray diffraction (XRD), X-ray photoelectron spectroscopy (XPS), scanning electron microscopy (SEM), N_2-physisorption, X-ray fluorescence (XRF), and H_2-temperature programmed reduction (H_2-TPR). The catalytic performances were evaluated using a fixed bed reactor with 5.5% n-pentane in air at 673 K and the liquid products were analyzed by a gas chromatography-mass spectrometry (GC-MS).

1.2 Objective of research

To study the effect of transition metal (Bi, Co, Fe, and Mn) doped on VPO catalyst for the partial oxidation of n-pentane.

1.3 Scope of research

1) Preparation of vanadium phosphorus oxides (VPO) by precipitation method.

2) Synthesis of transition metal doped on VPO catalyst by varying the kind of metal (Co, Bi, Fe, and Mn) by precipitation with H_3PO_4 and alcohol.

3) Studying the properties of VPO catalyst upon the addition of different concentration of the best metal from 2).

4) Catalyst characterization by many techniques such as X-ray powder diffraction (XRD), Surface Area and Porosity Analyzer (BET), scanning electron microscope (SEM), X-ray fluorescence (XRF) and X-ray photoelectron spectroscopy (XPS), and H_2-temperature-programmed reduction (H_2-TPR).

6) Reaction study of the promoted and unpromoted catalyst in the partial oxidation of n-pentane reaction in a stainless steel fixed-bed reactor under temperature 400 ^{o}C and atmospheric pressure.

1.4 Determining the chemical activity and products selectivity

Conversion and selectivity percentage in the partial oxidation of n-pentane reaction were estimated as follows;

1.4.1 Conversion of n-pentane

$$\text{Conversion (\%)} = \frac{\text{Area of n-pentane consumed}}{\text{Area of n-pentane in}}$$

1.4.2 Selectivity of liquid product

$$\text{Selectivity of MA (\%)} = \frac{\text{Liquid product weight} \times \text{The amount of MA in liquid product}}{\text{MA molecular weight} \times \text{Mole conversion}}$$

$$\text{Selectivity of PA (\%)} = \frac{\text{Liquid product weight} \times \text{The amount of PA in liquid product}}{\text{PA molecular weight} \times \text{Mole conversion}}$$

1.5 Research methodology

Part I: Synthesis of transition metal promoted on VPO catalysts by varying the kinds of the 2nd metal.

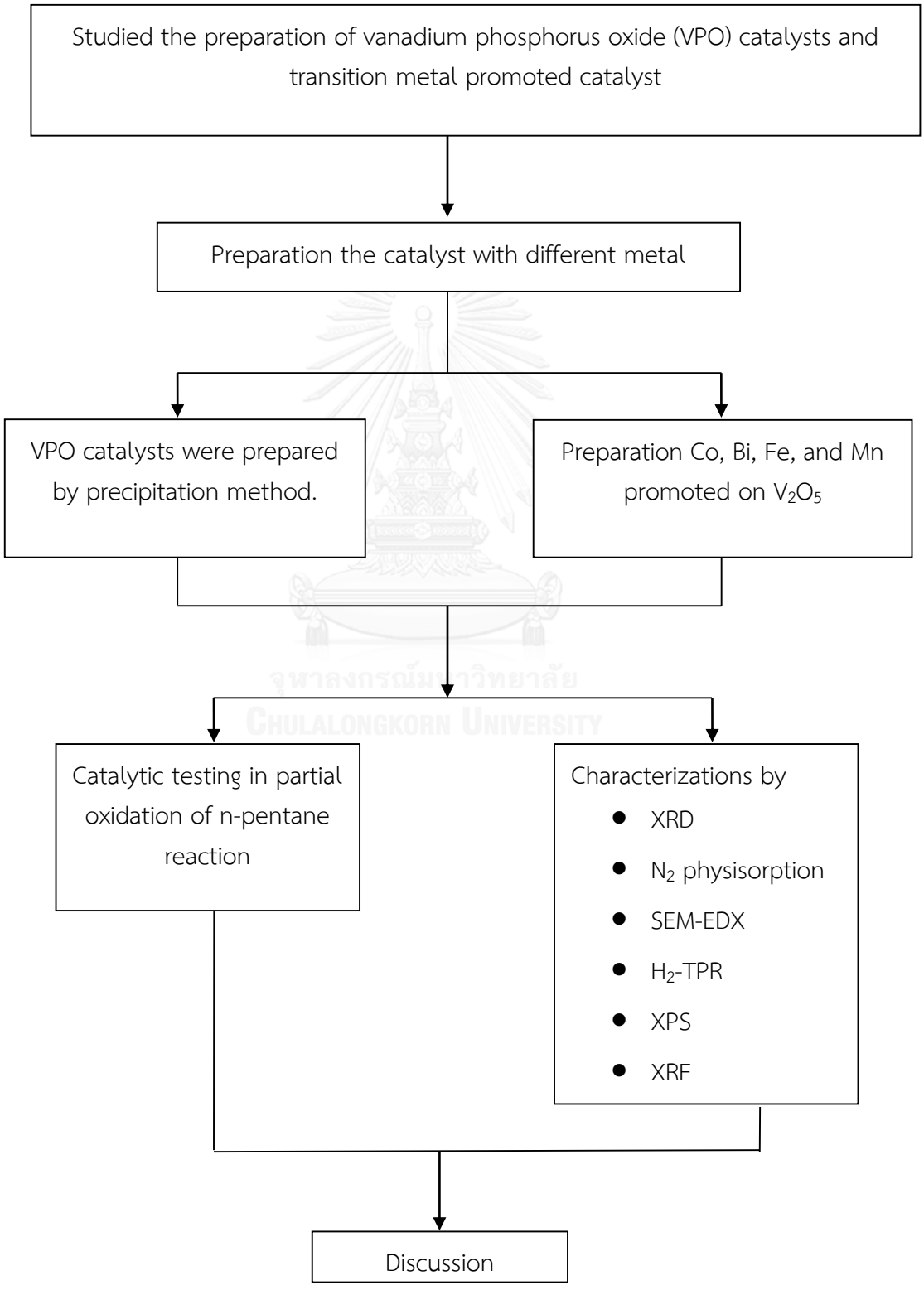

Part II: The catalyst activities comparison of different metal concentrations on VPO catalysts.

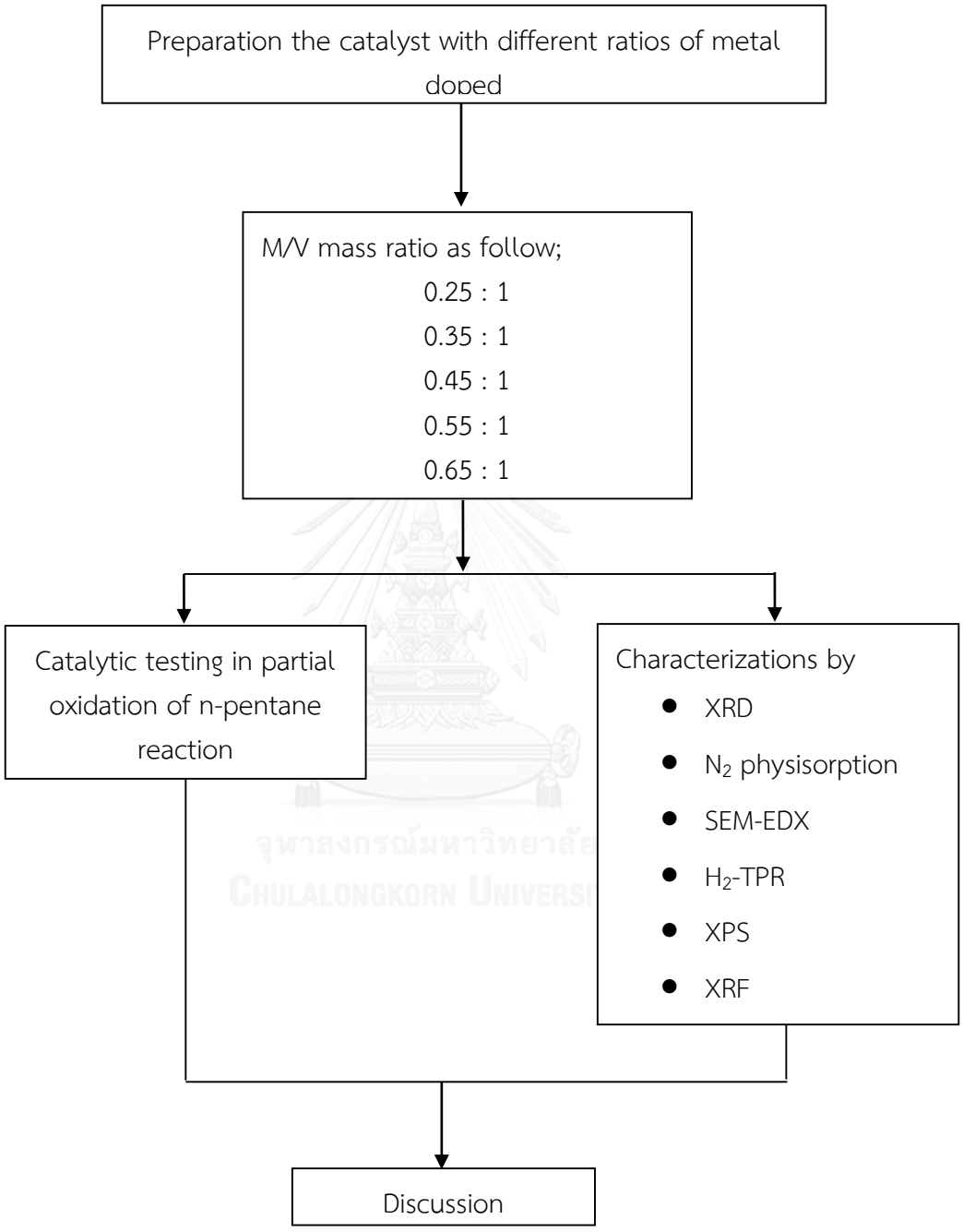

CHAPTER 2
THEORIES

2.1 Partial oxidation of n-pentane reaction

The feedstock for the global manufacture of maleic anhydride (MA) is benzene and n-butane. However, the scope of n-pentane as feedstock has been recently studied. Besides MA, phthalic anhydride is the product in the partial oxidation of n-pentane too. The partial oxidation of n-pentane over vanadium phosphorus oxide (VPO) catalyst is one of the most partial oxidation reactions and is highly exothermic reactions. The reaction of the selective oxidation of n-pentane to MA and PA is described below:

$$4C_5H_{12} + 15.5O_2 \longrightarrow 3C_4H_2O_3 + C_8H_4O_3 + 19H_2O$$

The partial oxidation of n-butane and n-pentane over VPO catalyst were similar and both proceeded through the formation of the corresponding olefins. But the production of PA indicated in a product of higher carbon number (C8) than low carbon atom. Although the two n-butane components would provide a sufficient number of carbon atoms but they cannot present the PA form [7]. The 1,3-pentadiene and pentene were the primary intermediate products in the partial oxidation of n-pentane. In addition to, pentadiene can be oxidizing to MA. Moreover, other section pentadiene can be changed to cyclopentadiene by dimerization, which was strongly adsorbed on the VPO catalyst surface. The strong adsorption of cyclopentadiene may give to the transformations between two adsorbed cyclopentadiene molecules. Thus an adsorbed intermediate with a higher carbon number and it can form the PA component [5, 7].

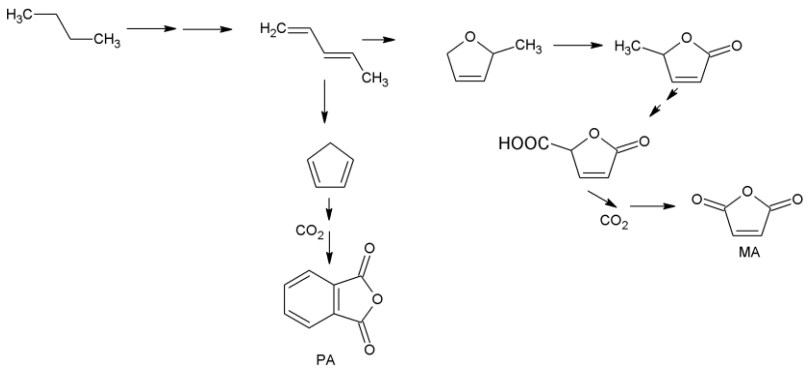

Figure 2.1 The partial oxidation of n-pentane to MA and PA mechanism [7].

2.2 Mechanism of partial oxidation

The partial oxidation product, MA is always more electronegative than the clusters, hence, any covalent interaction will proceed via base attack from surface of catalyst on acid sites in MA. Two alternative orientations for electrostatic alignment of MA at the active site is shown in Figure 2.2. =C–H hydrogens and C=O oxygens are the sites of the highest positive and negative charge, respectively. In Figure 2.2 a), C=C is shielded from surface base sites. The electronegativity gradient prevents electron transfer from C=O to vanadium. However, if MA with the orientation as shown in Figure 2.2 (b), electron donation from surface P–O oxygens and vanadium to the C=C carbons may initiate covalent chemisorptions [8]. PA is the product in n-pentane oxidation, which is made from the synthesis of the C_8 anhydride. It is a new type of oxidation reaction involving the formation of multiple C-C bonds and aromatization, an unusual effect in the presence of gaseous oxygen and an oxidation catalyst [9].

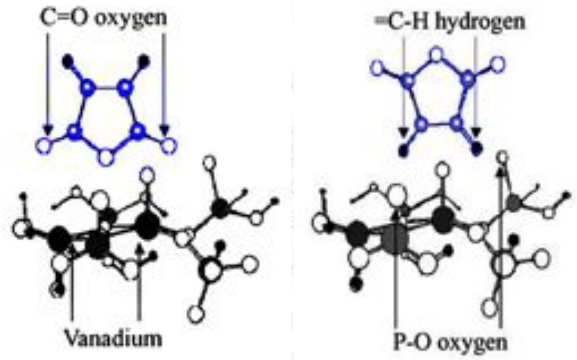

Figure 2.2 Two alternative orientations for electrostatic alignment of MA [8].

The primary role of vanadyl pyrophosphate is to oxidise n-pentane by removal of hydrogen and insert oxygen onto the four carbon chain. Ebner et al. [10] have focused on the determination of determine the roles of lattice and surface oxygen in the selective oxidation of n-butane via temporal analysis of products (TAP) reactor. And they have proposed that the initial activation is performed by surface oxygen, while the intermediate oxidation steps are performed by lattice oxygen. Moreover, Herrmann et al. [10] has make use of electrical conductivity measurements and proposed that O^- and O^{2-} are associated with V^{4+} and V^{5+}. He also further proved that V^{4+}–O^- pair are possible reactive oxygen species responsible for n-butane activation. On the other hand, Coulston et al. [11] has claimed that V^{5+}–O species is responsible

for the rate of MA formation directly. And other literatures also support that V^{5+}–O species is important in determination of the selectivity of catalyst.

2.3 Properties and structiure of MA and PA

2.3.1 Properties of MA

Maleic anhydride (MA) is an organic compound with the formula $C_2H_2(CO)_2O$ chemically 2,5 – furandione, and cis-butene-dioic anhydride. MA is also known by other names such as maleic acid anhydride, toxilic anhydride, etc. It is a white hygroscopic solid and forms orthorhombic crystalline needles. It is a solid at room temperature but is a liquid or gas during production. The physical properties of MA are shown in Table 2.1. MA, being an anhydride, is subject to hydrolysis to the acid on storage. Thus, to obtain a pure sample of MA, purification is necessary. It is purified commercially by distillation and it can be purified by sublimation or crystallization. Chloroform or aromatic solvents such as dimethyl sulfoxide (DMSO), benzene, toluene, and xylene are adequate as crystallizaing solvents [7]. MA was produced by the oxidation of n-pentane or other aromatic compounds.

Maleic anhydride is a composition in the production of unsaturated polyester resins. These laminating resins, which have good dielectric properties and high structural strength, have a variety of applications in automobile bodies, building, molded boats, chemical storage tanks, machinery housings, radar domes, lightweight pipe, and bathtubs, etc [7, 8].

Table 2.1 Physical properties of maleic anhydride (MA)

Physical properties of MA	Information
Molecular Weight	98.057 g/mol
Crystalline forms	Needles, rhombic
Flash point	Open cup 110°C (230°F)
	Closed cup 102°C (215°F)
Autoignition temperature	477°C (890°F)
Boiling point at 760 mmHg	202°C (395°F)
Density (water = 1.00)	Molten 1.3 g/cm^3 at 70°C
	Solid 1.48 g/cm^3
Melting point	52.8°C (127°F)
Solubility in water	Hydrolyzes slowly
Vapor density	3.38

MA is the anhydride of cis-butenedioic acid or maleic acid and the carboxylic acid groups next to cis form. It has a cyclic structure with a ring containing four carbon atoms and three oxygen atoms. In the crystalline state the molecule is essentially planar, with the oxygen atom in the five-membered ring lying 0.03 Å from the plane of the other atoms. The bond distances and bond angles are shown in Figure 2.2.

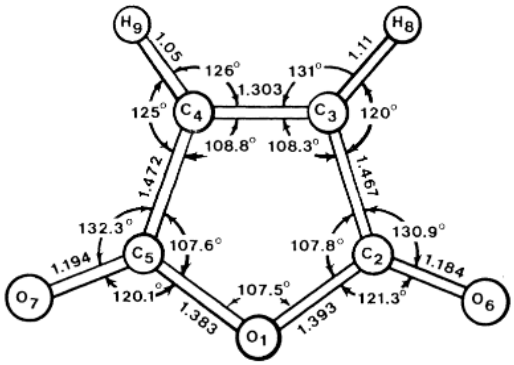

Figure 2.3 Bond distances and angles in maleic anhydride [7]

2.3.2 Phthalic anhydride

Phthalic anhydride (PA) is the organic compound with the formula $C_8H_4O_3$ or $C_6H_4(CO)_2O$. Other names of PA are Isobenzofuran, 1,3-dione, 1,3-Isobenzofurandione, and 1,3-Phthalandione, etc. The process begins with the reaction of PA such as partial oxidation of n-pentane reaction, the selective oxidation of o-xylene and alcoholysis reaction. PA is a white solid that is an important in chemical industry. It is as a chemical intermediate in the production of polyester resins, alkyd resins and plastics. Phthalate plasticizers are used for the production of flexible PVC products such as cables, pipes, hoses, leather cloth, shoes, and packaging film. Boiling point and melting point of PA are 285°C and 131°C, respectively. The structure and physical properties of PA is shown in Figure 2.3 and Table 2.2, respectively [3, 8].

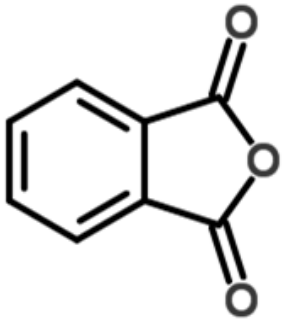

Figure 2.4 The structure of phthalic anhydride [9]

Table 2.2 Physical properties of PA [8]

Physical properties of MA	Information
Molecular Weight	148.117 g/mol
Flash point	152°C (305°F)
Autoignition temperature	570°C (1058°F)
Boiling point at 760 mmHg	285.3°C (563°F)
Density (water = 1.00)	1.53 g/cm³
Melting point	131°C (267°F)
Solubility in water	6,200 mg/L at 25°C
Vapor density	6.6 (Air = 1)

2.4 Vanadium phosphorus oxide catalyst

Catalyst based, on vanadium oxide are frequently used in the oxidation of light alkanes reaction due to high activity and selectivity. Phases compound in VPO catalyst include V^{5+}, V^{4+}, and V^{3+}, V^{5+} such as $VOPO_4$•H2O, β-$VOPO_4$, γ-$VOPO_4$, and δ-$VOPV_4$; V^{4+} such as VOHPO4•H2O and $(VO)_2P_2O_7$; and V^{3+} such as VPO_4 and $V(PO_3)_3$, etc. The active phase, that increase the high performance of VPO catalyst is vanadyl pyrophosphate ($(VO)_2P_2O_7$) [10].

2.4.1 structure of $(VO)_2P_2O_7$

Vanadyl pyrophosphate phase is an active phase in VPO catalyst and it can be transformed from $VOHPO_4$•$0.5H_2O$ by calcination. Vanadium phosphate hexahydrate is made from vanadium octahedral and phosphorus tetrahedral. VO_6 octahedral and PO_4 tetrahedral are connected and fromed to (0 0 1) planes. Water molecules are connected with 0 0 1 planes by hydrogen bonds. The coordination of vanadium

contains with oxygen dubble bond (V=O). The structure of (0 0 1) plane of $VOHPO_4{\cdot}0.5H_2O$ and $(VO)_2P_2O_7$ is show in Figure 2.4 and 2.5, respectively. The trans formation $VOHPO_4{\bullet}0.5H_2O$ to $(VO)_2P_2O_7$ occurs to be topotactic with 2 molecule of water elimination.

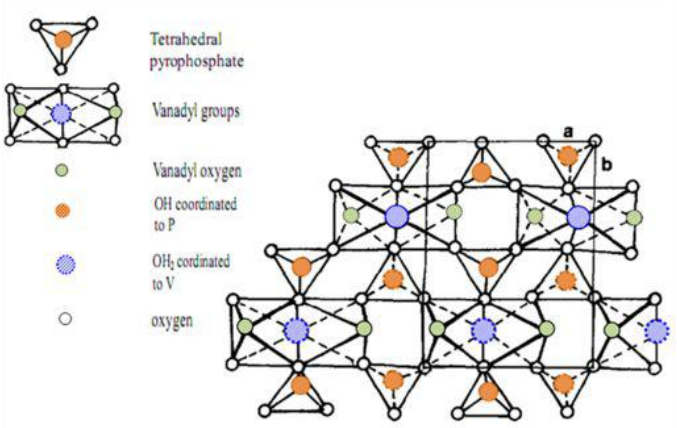

Figure 2.5 Idealised structure of (0 0 1) plane of $VOHPO_4{\cdot}0.5H_2O$ [10]

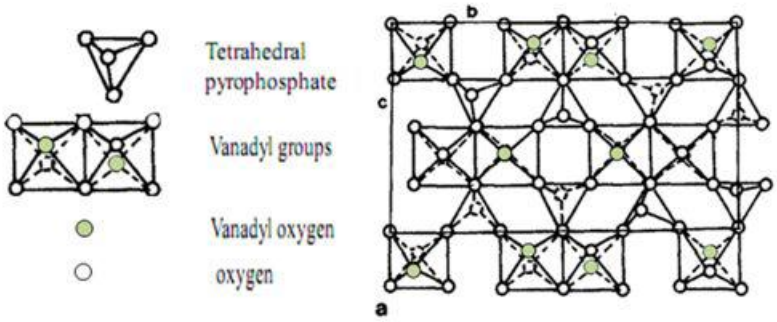

Figure 2.6 $(VO)_2P_2O_7$ structure [10]

2.4.2 Vanadyl phostate ($VOPO_4$) structure

$(VO)_2P_2O_7$ phase is readily oxidized to various phase of $VOPO_4$ such as αI, αII, and β-$VOPO_4$ phase. They are different from $(VO)_2P_2O_7$ due to structure and formation, these phase are maded from VO_6 octahedral single column connected with PO_4 tetrahedral. The structure of αI and αII-$VOPO_4$ are presented in Figure 2.6 a) and b), respectively. From Figure 2.6 a) and b), PO_4 tetrahedral shares four oxygen atoms with four different the vanadium coordination column that are parallel with each other atom. β-$VOPO_4$ phase has four of PO_4 oxygen atoms and it shared the oxygen atom with VO_6 octahedral in one column, other two oxygen atom shared with different VO_6 2 columns. The structure of β-$VOPO_4$ is shown in Figure 2.6c.

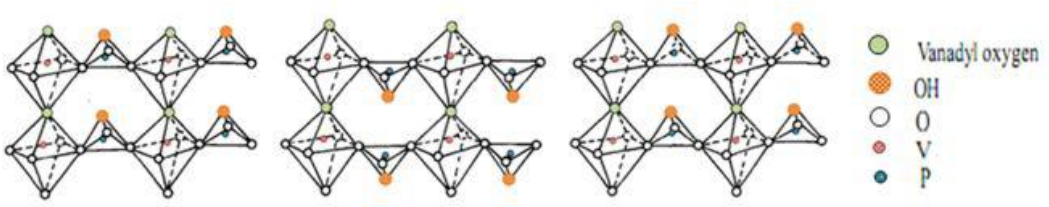

Figure 2.7 Structure of (a) αI-$VOPO_4$; (b) αII-$VOPO_4$; (c) β-$VOPO_4$ [10]

2.5 Precipitation method

The preparation of catalyst by precipitation is an important technique. These techniques have been used to produce catalyst with better performance and to compensate the higher cost of catalyst. The precipitation process has many ways to carry out. The simple processing of precipitation reaction is a batch operation when the solution is present in the precipitation flask. Then, precipitation agent is added and the last process is calcination of a precursor for displaced the impurities. A general flow scheme for a precipitated catalyst preparation is show in Figure 2.7 [11].

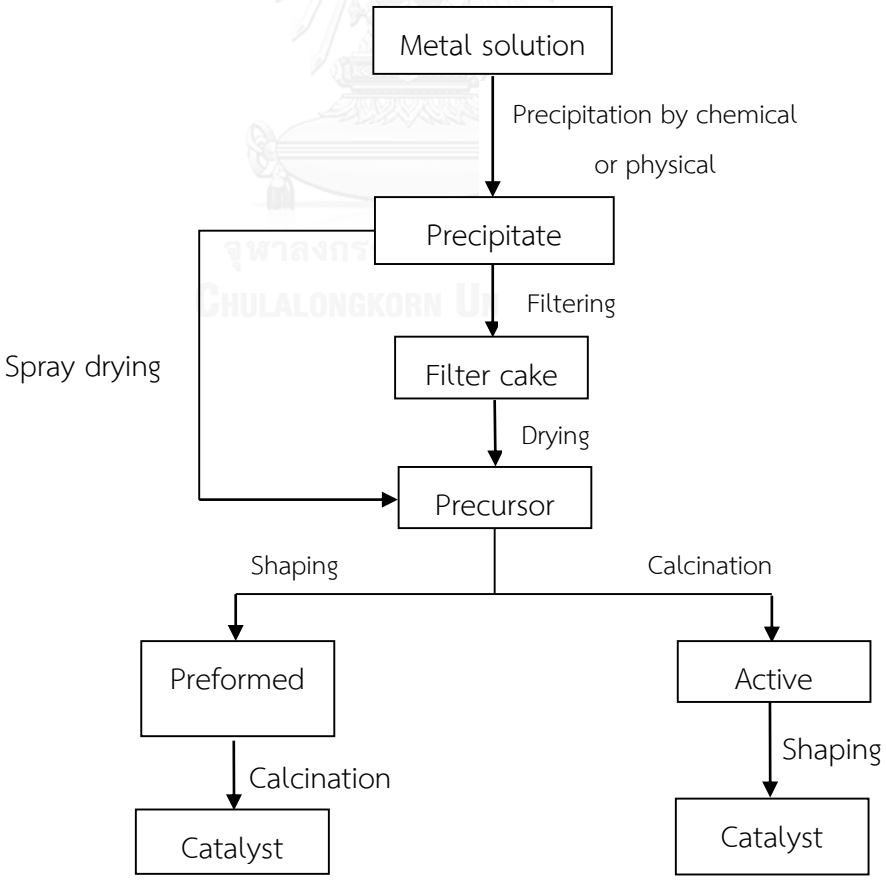

Figure 2.8 A general flow scheme for a precipitated catalyst preparation [11]

The formation of the precipitate occurs as a result of physical transformations that change of temperature, solvent and solvent evaporation. The chemical additions are acids and bases for forming agents. The chemical and physical properties of the precipitates that lead to an increase in the particle size of a precipitate. Because the solubility increases with decreasing particle size, small particles begin to dissolve and large crystals continue to grow.

As an example, two procedures can be summarized for the preparation of VPO catalysts for partial oxidation of n-pentane. One procedure is reduction of V_2O_5 in aqueous medium, followed by addition of H_3PO_4 or reduction of V_2O_5 in an organic medium, using isobutanol, butanol or ethylene glycol then followed by addition of H_3PO_4. The catalysts prepared in organic media are more active. In this example, the precursor acts as an improved matrix for the crystalline growth of the oxide active phase. The properties that the solid will develop as a final catalyst are strongly affected by all structural and morphological changes which occur during the topotactic transformation [11].

CHAPTER 3
LITERATURE REVIEWS

VPO catalyst has been studied in the partial oxidation of n-pentane reduction. Many papers have been taken into consideration about how to improve the performances of catalyst. An alternative factor which can greatly affect the catalytic performance is the addition of the metal promoter. The catalyst performances of VPO catalyst and the effect of metal loading in the selective oxidation of n-butane to MA and the partial oxidation of n-pentane to MA and PA are summarized in this chapter.

3.1 VPO base catalyst

Ali, A. et al. (2009) [12] presented the high surface area vanadium phosphate catalyst for n-butane oxidation. The aim of this research was to study the effects of alcohol solvents, water treatment, and microwave heating with catalytic performance. Reducing agents or alcohol solvent for catalyst preparation was isobutyl alcohol, 1-butanol and ethylene glycol, and thermal treatment used conventional heating and microwave heating. In the part of catalytic testing, n-butane oxidation was carried out in a fixed bed reactor at 673 K with GHSV of 2400 h^{-1}. 1.7% n-butane in air was flow via 0.25g of catalyst bed and gas products were detected by online gas chromatography. The catalysts were refluxed with distilled water and dried with microwave heating had higher specific surface area. Moreover, type of the reducing agent had a strong impact on the catalyst properties.

Xiao, B. et al. (2012) [13] investigated the preparation of vanadium phosphate precursor for the selective oxidation of butane using α,ω-alkanediols. In this work, the effect of various the reducing agent such as isobutanol, 1,4-butanediol, 1,5-pentanediol, and 1,6-hexanediol was studied. The catalyst was prepared by precipitation method and main strategy for the synthesis of catalyst was a mixture of V_2O_5 and H_3PO_4 with isobutanol and α,ω-alkanediols. It was found that the size of d (0 0 1) plane increased, when the carbon number of α,ω-alkanediols increased. The catalyst prepared by isobutanol and 1,4-butanediol had higher surface area, small size and comprised of V^{5+} and V^{4+} phase, so the activity and selectivity of catalyst were increased.

Bignaradi, G. et al. (2006) [5] showed an improved relationship between the oxidation state of vanadium in catalyst and the product distribution in the oxidation of n-pentane. Higher amount of V^{5+} led to the increasing of MA due to the crystallinity of VPO catalyst was an important factor. The reduced oxidation state of catalyst made the products selectivity decreased.

3.2 Transition metal promoter

Zazhigalov, V. et al. (2002) [14] reported the effect of bismuth additives on the properties of vanadium phosphorus oxide catalyst in the partial oxidation of n-pentane. The flow rate of 1.6% of n-pentane was varied from 12-46 ml/min and the temperature was varied from 180°C to 480°C. Bismuth was added with V_2O_5 and organic solvent, the ratio of Bi/V was ranged from 0 to 0.30 and P/V ratio was 1.15. The addition of Bi to the VPO catalyst produced in an increase the amount of adsorbed base or increase number of acidity sites and when the surface acidity increased the selectivity of MA and PA increased. MA and PA selectivity were higher due to the increasing of Brønsted and Lewis acidity, respectively. The best temperature and Bi/V ratio, which gave the higher activity and selectivity, were 400°C and 0.3, respectively.

Taufig, Y. et al. (2006) [15] mentioned the modification of vanadyl pyrophosphate ($(VO)_2P_2O_7$) phase by the addition of bismuth on undoped catalyst in n-butane oxidation. Bi promoted catalyst compared with unpromoted catalyst, had higher specific surface area than the unpromoted catalyst. Surface area of unpromoted and promoted catalyst was 20.3m^2/g and 25.0m^2/g, respectively. Furthermore, Bi promoted catalyst gave a higher compact structure and affected the rosette shape of d (0 0 1) plane increase. So, all of factors generated highly activity and selectivity.

Goh, C. et al. (2008) [16] compared the performances of the catalysts prepared by different preparations, i.e. (i) Bi and Fe doped in the refluxing $VOPO_4•2H_2O$ with isobutanol, (ii) the addition of Bi-Fe in the synthesis of $VOHPO_4•0.5H_2O$, and (iii) the reducing agent treatment of VOHPO4•0.5H2O and Bi-Fe oxide in alcohol. The best catalyst performance was prepared by (ii) method. This method gave a higher activity, although it had a lower specific surface area but it had a higher the amount of V^{4+} state. n-Butane conversion and MA selectivity of catalyst were 72% and 61%, respectively.

Cabani, F. et al. (1997) [6] investigated the effect of cobalt and iron doped on the catalytic behavior of VPO catalyst in the selective oxidation of n-pentane to MA and PA. This research used isobutanol as reducing agent. The catalyst results indicated the modification of Co dopping on VPO catalyst could increase the performance of catalyst, when compared with Fe dopping. That Fe promoter hindered the crystallization of $(VO)_2P_2O_7$ phase and intercepted the vanadium IV state too. Furthermore, the catalyst doped with Fe led to decrease the selectivity of PA but it increased the selectivity of CO_x.

Andrea, M. et al. (2002) [17] studied, vanadium phosphorus oxide catalyst modified by niobium (Nb) doping for mild oxidation of n-butane to MA. This work showed the development of strong Lewis acid sites with addition Nb on VPO catalyst. The increment of Nb doped on VPO catalyst affected the increase in the number of O-vacancies and support the initial activation of C-H in reactant. Apart from that, the amount of O-vacancies had made strong Lewis acidity in low temperature of desorption but weak in high temperature due to the structure of catalyst destroyed. From electron microscopy (TEM) analysis the $(VO)_2P_2O_7$ crystallinity of Nb promoted catalyst was lower than unpromoted catalyst, but Nb promoted catalyst had the rosette platelets more than VPO catalyst. The conversion and selectivity of Nb dopped catalyst at 400^{o}C were 75% and 71%, respectively. While, the conversion and selectivity of VPO undoped catalyst were 58% and 70%, respectively.

Taufiq, Y. et al. (2010) [18] investigated the Effect of Cr, Ni, Fe, and Mn dopants on the performance of hydrothermal synthesized vanadium phosphate catalysts for n-butane oxidation. The VPO catalyst was synthesized by hydrothermal technique and different metals were doped such as Cr, Ni, Fe, and Mn. The results showed that the addition of metal into the VPO catalyst increased the specific surface area. Moreover it changed the structure of the catalyst with reducing $(VO)_2P_2O_7$ to $VOPO_4$, indicating the transformation of V^{4+} to V^{5+} phase. However, the addition of metal promoter on VPO catalyst showed improved performances of catalyst. The sequence of n-butane conversion, for the different metal dopants from most to least was: Cr > Mn > Fe > VPO > Ni doped catalyst.

Cheburakava, E. et al. (2007) [19] presented the effect of metal doped on VPO catalyst with acid sites. The PA selectivity can be achieved by increase the number of Lewis acidity but that also decrease the selectivity of MA. Sort of the amount of Lewis acid sites in metal promoter from large to small was Ti, Fe, Zr, and Mo, respectively.

3.3 The metal oxide supports

Taufiq, Y. et al. (2007) [20] studied the physical and chemical of VPO supported on γ-Al_2O_3 that affected the catalytic performance. The catalyst precursor was prepared by precipitation method and was impregnated onto γ-Al_2O_3 using wetness impregnation technique. γ-Al_2O_3 support was used as an inert compound to disperse active phase and it can increase the specific surface area of catalyst to achieve a higher activity. From the results, it was found that the conversion of n-butane decrease when V^{4+} was transformed to V^{5+}.

Sooboo, S. (2016) [1] investigated the amount of MA and PA, when vanadium phosphorus oxide was loaded on hydroxyapatites (HAp) by wet-impregnation technique. From the catalytic results, the increment of VPO loading on the HAp support increased the conversion of catalyst about 75% and more increase of the primary products because $(VO)_2P_2O_7$ phases were increased. The best temperature in this reaction was 360^{o}C.

Table 3.1 Summary of the research on n-butane selective oxidation by various catalysts

Catalyst	Metal promoted	solvent	n-Butane convertion (%)	Selectivity of MA (%)	condition	T_r (°C)	Ref.
VPO	-	1) isobutanol	52	56	1.7% n-butane was flow via 0.25 g catalyst bed with a GHSV 2400 h^{-1}.	400	[12]
		2) 1-butanol	45	68			
		3) ethylene glycol + water tretment	65	74			
VPO	-	1) isobutanol	50	58	1.7% butane in air fed at 10 ml/min and contained 0.2g of catalyst for 72 h.	400	[13]
		2) 1,4-Butanediol	44	36			
		3) 1,5- Butanediol	20	24			
		4) 1,6- Butanediol	15	22			
VPO	M/V = 0.005	oxalic acid dihydrate	15	29	0.88%n-Butane in air to MA was carried out in a fixed-bed reactor and packed 0.25 g of catalyst.	150	[18]
Ni			12	23			
Fe			18	27			
Mn			23	32			

Table 3.1 (cont.) Summary of the research on n-butane selective oxidation by various catalysts

Catalyst	Metal promoted	solvent	n-Butane convertion (%)	Selectivity of MA (%)	condition	T_r (°C)	Ref.
VPO	Bi	isobutanol	65	75	1.5 vol% of n-butane was introduced in reactor at rate of 10 ml/min.	430	[15]
1% Bi			70	68			
3% Bi			70	76			
VPO	1% and 2% Bi and Ni loading	isobutanol	38	28	Feedstock composition of 1% n-butane in air was fed to a fixed-bed micro reactor with a GHSV = 2400 h-1.	400	[21]
			52	39			
			52	37			
			51	36			
VPO bulk	M/V = 0.005	butanol	58	45	1g of catalyst was packed in a fixed bed microreactor. 1.5% n-butane was flow via reactor bed with a GHSV = 900 h^{-1}.	330	[22]
1.5%Co			51	48			
VPO	Si, Ti	butanol	20	35	1.2% n-Butane in air fed into reactor (1 g of catalyst).	400	[23]
0.25%Si			23	47			
0.25%Ti			13	16			

Table 3. 2 Summary of the research on n-pentane partial oxidation by various catalysts

Catalyst	Metal promoted	solvent	n-Putane Conversion (%)	Selectivity of MA (%)	Selectivity of PA (%)	condition	T_r (^oC)	Ref.
VPO	-	isobutanol	90	60	10	1.7% n-butane was flow via 0.25 g catalyst bed with a GHSV 2400 h^{-1}.	400	[5]
Bi:V = 0.1	Bi	isobutanol	27	36.6	26.1	1.7% butane in air fed at 10 ml/min and contained 0.2g of catalyst for 72 h.	400	[14]
0.2			37.5	35.7	29.8			
0.3			35.9	41.4	22.5			
0.35			24.7	44.7	15.4			
VPO/Al_2O_3			2	76	3	0.88%n-Butane in air to MA was carried out in a fixed-bed reactor and packed 0.25 g of catalyst.	300	[24]

Table 3.2 (cont.) Summary of the research on n-pentane partial oxidation by various catalysts

Catalyst	Metal promoted	solvent	n-Putane Conversion (%)	Selectivity of MA (%)	Selectivity of PA (%)	condition	T_r (^oC)	Ref.
VPO	Fe, Co	isobutanol	22	39	32	n-Pentane 1% in air	340	
Fe : V = 0.016			23	29	45	was flow into 1g		
Co : V = 0.0102			14	38	22	catalyst.		[6]

CHAPTER 4
EXPERIMENTAL

Vanadium phosphorus oxide (VPO) catalysts were promoted with different transition metals (M = Co, Bi, Fe, and Mn) for the partial oxidation of *n*-pentane. This chapter is divided into 3 parts; the first part is the preparation of VPO and transition metal doped on VPO catalysts. The second part is catalysts characterization techniques such as X-ray powder diffraction (XRD), Surface Area and Porosity Analyzer (BET), scanning electron microscope (SEM), X-ray fluorescence (XRF) and X-ray photoelectron spectroscopy (XPS). The final part is the catalytic testing.

4.1 Catalysts preparation

4.1.1 Preparation of vanadium phosphate (VPO) catalyst

1) Synthesis of $VOPO_4 \cdot 2H_2O$

Vanadyl phosphate dihydrate ($VOPO_4 \cdot 2H_2O$) catalyst was prepared by reacting, vanadium (V) pentoxide (V_2O_5) 8 g with aqueous 85% ortho-phosphpric acid 38.3 ml and distilled water (24ml H2O/g solid). The mixtures were refluxed 6 rpm and heated to 120 ^{o}C for 16 h. Then, the yellow solid was separated by vacuum filtration and washed with distilled water and acetone (100 ml the both of them). After that, the result cake was filtrated and dried with oven at 120 ^{o}C for 16 h under ambient atmosphere [12].

2) Synthesis of $VOPO_4 \cdot 0.5H_2O$ and VPO catalyst

Vanadyl hydrogen phosphate hemihydrate ($VOHPO_4 \cdot 0.5H_2O$) was synthesized by adding $VOPO_4 \cdot 2H_2O$ from step 1) 2 g to ethylene glycol 80 ml. The mixture was refluxed for 16 h on time and then, separated the blue solid with vacuum pump. Distilled water and acetone washed green-blue solid and dried with oven at 120 ^{o}C for 16 h. Finally, 2 g of precursors were stirred distilled water for 2 h without heating and dried them with oven at the same condition. The resulting catalyst was denoted vanadium phosphate (VPO) catalyst [12].

4.1.2 Preparation of transition metal promoted catalysts

The different metals have been used as the modifier, and data has been published on their influence on selectivity of maleic and phthalic anhydride, and on the reaction rate of these catalysts. Transition metals (M) were used in this research that was cobalt (Co), iron (Fe), bithmus (Bi), and manganese (Mn). First of all, the transition metal was doped on V_2O_5 (vanadium (V) pentoxide) 2 g, the P/V ratio and the M/V ratio was 1.15 and 0.35, respectively. The mixer powder was suspended by stirring in iso-butanol for 1 h at 120^{o}C, after that, added a ortho-phosphpric acid 85% stirring 1.5 rpm at 93 ^{o}C for 10h. The green-blue solid was filtered by vacuum filtration and washed the catalyst precursor with iso-butanol 250ml and acetone 100 ml respectively. The calcination of catalyst precursor was obtained at 300 ^{o}C (rate 10^{o}C/min). Finally, the resulting catalyst was denoted MV catalyst [14].

4.2 Catalysts characterization

4.2.1 X-ray powder diffraction (XRD)

The X-ray diffraction was a technique in determination of crystallinity and morphology of catalyst. XRD analyses in this research were carried out using SIEMENS D 5000 X-ray diffractometer with CuK_α (λ = 1.54439 Å) in the 2θ range of 10^{o} to 60^{o}.

4.2.2 N_2 physisorption

The total surface area, pore volume, pore size distribution of the catalysts precursor were analyzed by the BET method using nitrogen adsorption. This work used the micromeritics ASAP 2000 automated system.

4.2.3 Scanning electron microscope and energy dispersive x-ray spectroscopy (SEM-EDX)

SEM images were taken by JEOL mode JSE-6400 Scanning electron microscope and Link Isis Series 300 program energy dispersive x-ray spectroscopy determined elemental distribution. The samples of catalyst were coated with gold using a Sputter Coater.

4.2.4 X-ray fluorescence (XRF)

Wavelength dispersive X-ray fluorescence spectrometry method was used to determine metals elemental that were doped on VPO catalyst. Elementals analyses were measured by using X-ray fluorescence spectrometer, Bruker model S8 Tiger.

4.2.5 X-ray photoelectron spectroscopy (XPS)

X-ray photoelectron spectroscopy (XPS) was used to measure the elemental identification and chemical oxidation state of element and was determined using an AMICUS photoelectron spectrum spectrometer, which analyzed by an MgKα X-ray as primary excitation and KRATOS VISION II software.

4.2.6 Temperature programmed reduction (H_2-TPR)

The H_2-TPR measurements were measured using a Micromeritics pules chemisorp 2750 instrument. The catalyst 0.1 g was packed in quartz bed and heated to 200^{o}C for removed any adsorbed by N_2 gas flowed 25 ml/min. After cool down, Feed 10%H_2/Ar (25 ml/min) and heat up to 800^{o}C for determined the reducibility and calculated the area between TCD signal and time.

4.3 Partial oxidation of n-pentane reaction

The catalyst precursors were tested for the selective oxidation of n-pentane. Maleic anhydride and phthalic anhydride was the main product, primary product were carbon monoxide (CO) and carbon dioxide (CO_2). The reaction occurred in a continuous flow reactor placed inside a cylindrical furnace. The schematically instrument of reaction was shown below in Figure 4.1. The partial oxidation of n-pentane was carried out at 400^{o}C in a stainless steel fixed-bed reactor with an inside diameter of 3 mm. 0.3 g of catalyst and 0.07 g of quart wool were used for catalytic tests. 5.5% n-Pentane in air was fed to the reactor via mass flow controllers and was balanced with helium (Ultra high purity grade). Total flow in this reaction was 60 ml/min and reaction time was 3 h. Gas products were analyzed using gas chromatography detected by FID and TCD detector. After three hours, the liquid product was analyzed by gas chromatography mass spectrometry (another name was GC-MS). Maleic anhydride (MA) and phthalic anhydride (PA) were analyzed and separated by rtx 5 column.

Molecularsieve 5A column was used to analyze carbon dioxide (CO) and porapak Q was analyzed carbon monoxide (CO_2), the conditions was shown in Table 4.1.

Table 4.1 The conditions in gas chromatography

Gas chromatograph	Conditions			
Detector	FID	TCD	TCD	GC-MS
Column	rtx 5	molecular sieve 5A	porapak Q	MS
Carrier gas	H_2 and Ar	Ar	He	He
Inject temperature (°C)	300	80	100	300
Detector temperature (°C)	100	50	40	250
Column temperature (°C)	200	50	40	35-250

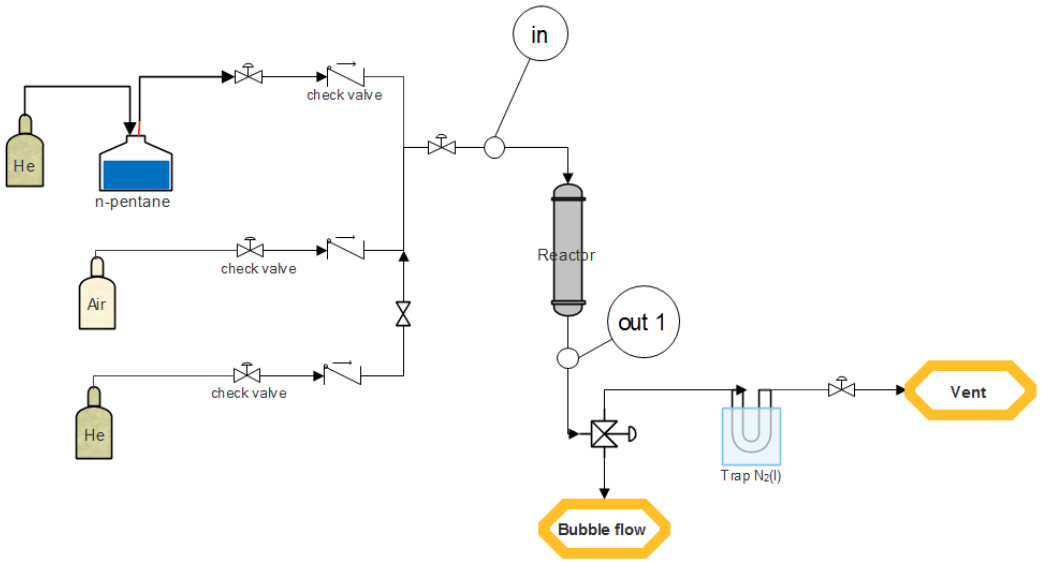

Figure 4.1 Schematic diagram used for catalytic testing of the partial oxidation of n-pentane.

CHAPTER 5
RESULTS AND DISCUSSION

The characterization and catalytic performance are presented in this chapter. The result and discussion are divided into two parts. The effect of transition metal (Co, Bi, Fe, and Mn) promoted on VPO catalysts was studied in the first part. In the second part, the catalytic activities of different metal concentrations on VPO catalysts were discussed. The catalysts were studied in the partial oxidation of n-pentane to MA and PA at 400°C and analyzed by X-ray powder diffraction (XRD), scanning electron microscopy (SEM) with energy dispersive X-ray analysis (EDX), temperature programmed reduction (H_2-TPR), X-ray fluorescence (XRF), X-ray photoelectron spectroscopy (XPS), and N_2-physisorption.

Part I

Synthesis of transition metal promoted on VPO catalysts by varying the kinds of the 2nd metal.

5.1. XRD

The structure and crystallization of unpromoted and promoted catalyst were studied by XRD analysis and are shown in Figure 5.1. The XRD patterns of the unpromoted VPO and promoted catalysts show the characteristic peaks of vanadyl phosphate dehydrate phase ($VOPO_4 \bullet 2H_2O$) at 2θ = 11.89°, which corresponded to the reflection of plane (0 0 1). The intensity of the peak at 2θ = 11.89° was enhanced upon calcination [17]. The main peaks at 2θ = 22.9, 28.4, 33.8, 43.2, and 58.4°, indicate the presence of vanadyl pyrophosphate phase ($(VO)_2P_2O_7$), which corresponded to (0 2 0), (2 0 4), (1 0 6), (0 0 8), and (3 1 9) plane, respectively [21, 30]. The addition of transition metal (Co, Bi, Fe, and Mn) into V_2O_5 promoted the formation of $(VO)_2P_2O_7$ (V^{4+} state) of the catalysts. It has been suggested that this phase was the active phase for the partial oxidation of n-pentane reaction, which resulted in higher activity and selectivity [20, 26]. Moreover, $(VO)_2P_2O_7$ phase was obtained by reduction of $VOPO_4 \bullet 2H_2O$ and $VOPO_4 \bullet 0.5H_2O$ phase using alcohol and oven heated [17, 18]. Additional peaks emerged at 2θ = 24.9 and 29.1, corresponded to the α-$VOPO_4$ phase. Such results indicate that the addition of these 2nd metals led to the formation of V^{5+} too [23].

The Co promoted on V_2O_5 also showed low intensity of (0 0 1) plane and an increased intensity of (2 2 1) plane because the hydrated phase transformed into an average valence state between V^{4+} and V^{5+} [6]. The addition of Bi into the catalyst led to the reflection at 2θ = 22.9° which corresponded to (0 2 0) plane [26, 31]. The Fe promoted catalyst exhibited the peaks at around 2θ = 21.9° and 22.9° which could be indicative of α-$VOPO_4$ and $(VO)_2P_2O_7$, respectively [6, 21]. The introduction of Mn into V_2O_5 led to change of the catalytic structure with reducing the reflection at 2θ = 11.8° but increasing the reflection peaks at 2θ = 22.9° and 28.4°. Both of the reflection at 2θ = 22.9° and 28.4° were the $(VO)_2P_2O_7$ active phase, which promoted the catalytic performances in the partial oxidation [23].

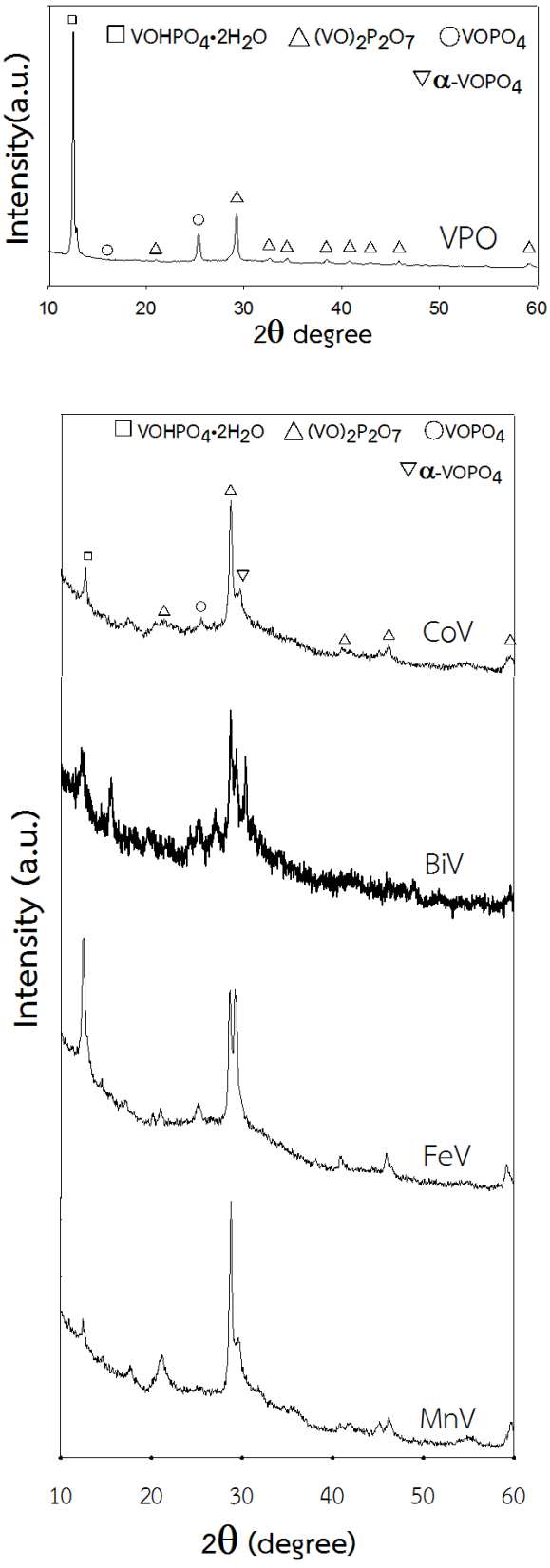

Figure 5.1 XRD patterns of unpromoted and transition metal promoted catalysts

5.2. Specific surface area and metals elemental measurements

The specific surface area of catalysts was measured by the Brunauer Emmett Teller (BET) method using a micromeritics ASAP 2000 automated system. The BET surface areas and the XRF results of unpromoted and promoted catalysts are summarized in Table 5.1. The Co, Bi, Fe, and Mn doped catalyst had a higher surface area than VPO undoped catalyst. The specific surface area of CoV, BiV, FeV, and MnV were determined to be 12.4, 7.4, 26.6, and 10.2 m^2/g, respectively, and that of VPO was determined to be 3.54 m^2/g. It was suggested that some amounts of the transition metals may be intercalated between the layers of crystal plate and produced a higher surface area [15, 21]. Yep et al. [25] suggested that the metal cations promoted on VPO catalyst were incorporated into interlayer spacing, resulting in a decrease of the weak H bond of phosphate and water in $VOHPO_4 \bullet 2H_2O$ phase. The (0 0 1) plane of the $VOHPO_4 \bullet 2H_2O$ was reduced, which led to the increase both of surface area and the intensity of (0 2 0) plane of $(VO)_2P_2O_7$ phase. This was consistent with the results from XRD analyses, that the surface area increased as the crystallite size decreased. Furthermore, the polarity and type of an alcohol that used as the reducing agent, may also have a strong impact on catalytic surface area, as well [12, 20]. All the samples exhibited negligible amounts of micro pore surface area.

Table 5.1 The BET surface areas of unpromoted and promoted catalysts.

Catalyst	N_2 physisorption results		
	BET surface area (m^2/g)	Pore volume ($x10^{-1} cm^3/g$)	Average pore diameter (nm)
VPO	3.5	0.07	18.7
CoV	12.4	0.24	11.4
BiV	16.3	0.23	13.3
FeV	26.6	1.04	12.0
MnV	10.16	0.26	13.1

The chemical compositions of catalysts were determined by X-ray fluorescence (XRF) analyzer and are shown in Table 5.2. The P/V and M/V ratios in the transition metal doped V_2O_5 were 1.15 and 0.35, respectively. The chemical compositions were confirmed by using the XRF technique. The P/V (phosphorus/vanadium) and M/V (metal promoter/vanadium) values for unpromoted and promoted catalysts are shown

in Table 5.1. The P/V ratio was 0.54 for VPO unpromoted catalyst and the P/V ratio for CoV, BiV, and FeV promoted catalyst were 0.57, 0.36, and 0.64, respectively.

The chemical analyses confirmed the presence of metal into V_2O_5 catalysts with the M/V atomic ratio of 0.18, 0.32, and 0.12 for CoV, BiV and FeV, respectively. However, an absent component of vanadium, phosphorus, and metal could occur by water and calcination treatment. The ratios between metal promoter and vanadium had an effect on the formation of different crystal planes and morphology of catalysts, As a consequence, it affected the surface area of catalysts.

Table 5.2 Chemical compositions of VPO unpromoted and promoted catalysts

Catalyst	EDX analyzed (wt%)			Mass ratio of EDX		XRF analyzed (wt%)			Mass ratio of XRF	
	V	P	M*	P/V	M/V	V	P	M	P/V	M/V
VPO	60.8	39.2	-	0.64	-	33.0	17.9	-	0.54	-
CoV	48.4	40.2	11.4	0.83	0.23	30.1	17.2	5.4	0.57	0.18
BiV	50.6	39.9	9.5	0.78	0.18	33.5	12.3	10.9	0.36	0.32
FeV	47.3	42.6	10.1	0.9	0.21	29.1	18.7	3.6	0.64	0.12
MnV	48.6	38.8	12.6	0.79	0.25	n/a	n/a	n/a	n/a	n/a

* M is the metal promoter

5.3. Scanning electron microscope and energy dispersive x-ray spectroscopy (SEM-EDX)

The results of chemical composition from EDX are illustrated in Table 5.2 with XRF evaluation. The chemical composition of VPO and metal promoted catalysts were analyzed by EDX. Higher weight percents of the elements from EDX than the XRF results were observed. That is the normal problem because the analysis of composition element by XRF would detect overall of bulk catalyst, whereas the SEM-EDX analyzed the composition by sample surface detection. The M/V ratios of CoV, BiV, FeV, and MnV from SEM-EDX were 0.23, 0.25, 0.18, and 0.25, respectively.

The surface morphologies of the unpromoted VPO and the transition metal promoted catalysts are illustrated in Figure 5.1. The structure of catalyst was similar and shown as thin plate-like crystals, which were agglomerated into the characteristics of rosette-shape clusters [13, 20]. The promoted catalysts showed higher compact and smaller size of crystal structure than the unpromoted catalyst. These crystals were made from agglomerates of $(VO)_2P_2O_7$ platelets with the preferentially exposed (1 0 0) crystal planes [15, 27]. Furthermore, the amorphous part in the form of small and flat particles with a secondary structure of catalyst plate may present due to the effect of high alcohol chain used in the preparation procedure [4]. In this research, isobutanol was used as the reducing agent. In Figure 5.1 (a) presents the SEM micrographs for VPO catalyst with a magnification of 5000 and 2000 SE. Relatively large thin sheets were observed. Wong et al. [27, 28] illustrated the SEM micrographs of $VOPO_4 \bullet 2H_2O$ and suggested that large plates stacked up to form to the layer structure may lead to a low surface area of VPO catalyst. The morphologies of Co doped catalyst are shown in Figure 5.1 (b). The Co promotd catalyst had smaller platelet morphology than the unpromoted VPO. The lamellar morphology of the crystals were developed from reducing $VOHPO_4 \bullet 2H_2O$ and enhanced agglomerates of $(VO)_2P_2O_7$ phase [29]. The morphologies of the Bi doped catalyst were similar to those of Co doped catalysts, as shown in Figure 5.1 (c). A higher compact structure had more layered plate as the crystals which were formed at the surface of catalyst clusters. The layered structure was mentioned to be the exposure of the (1 0 0) plate for $(VO)_2p_2O_7$ phase [21, 30]. In addition, the small size of the rosette clusters could result in a higher surface area.

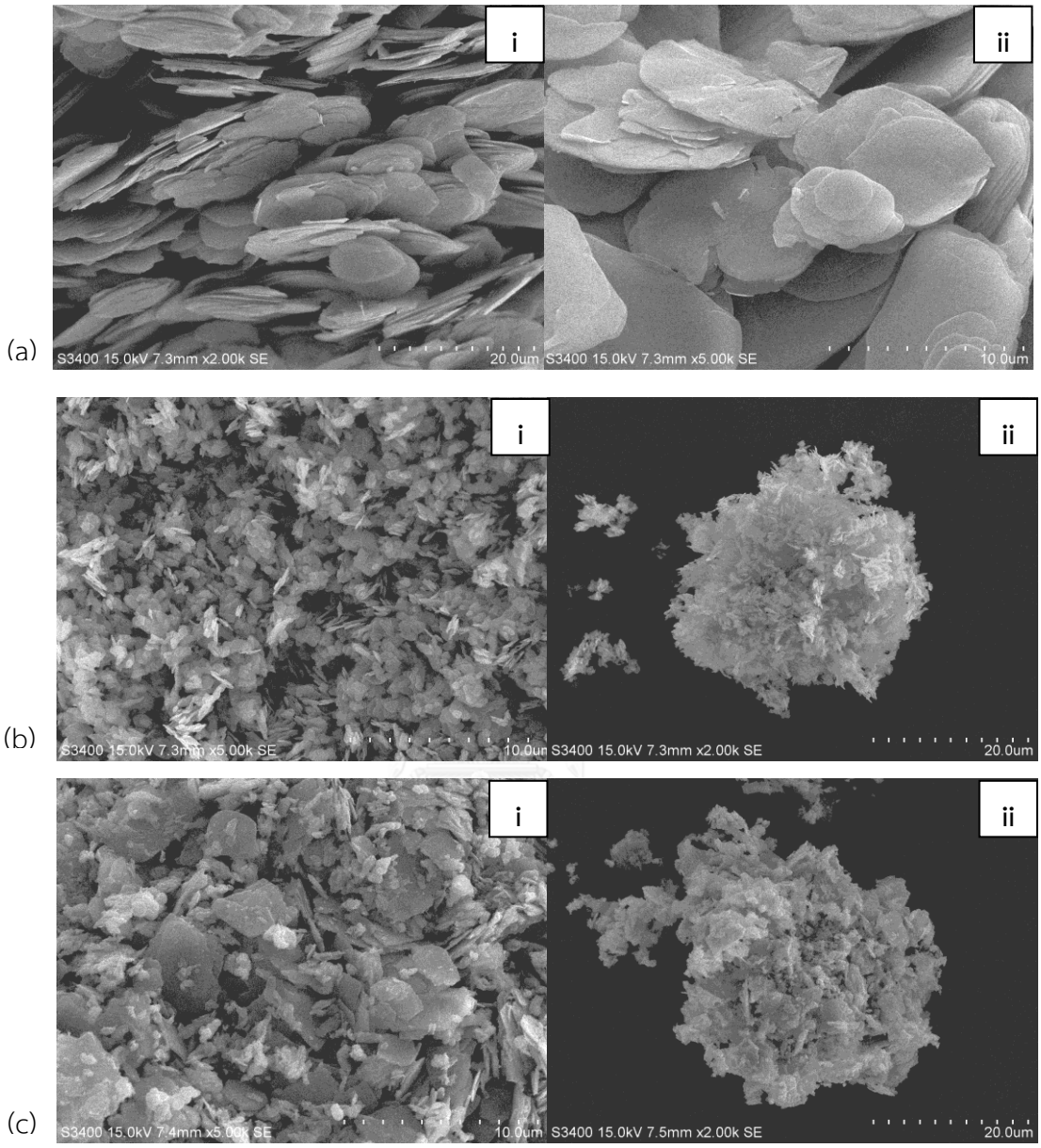

Figure 5.2 SEM micrographs for (a) bulk VPO; (b) CoV and (c) BiV catalyst; When (i) ×5000 (ii) ×2000

(d)

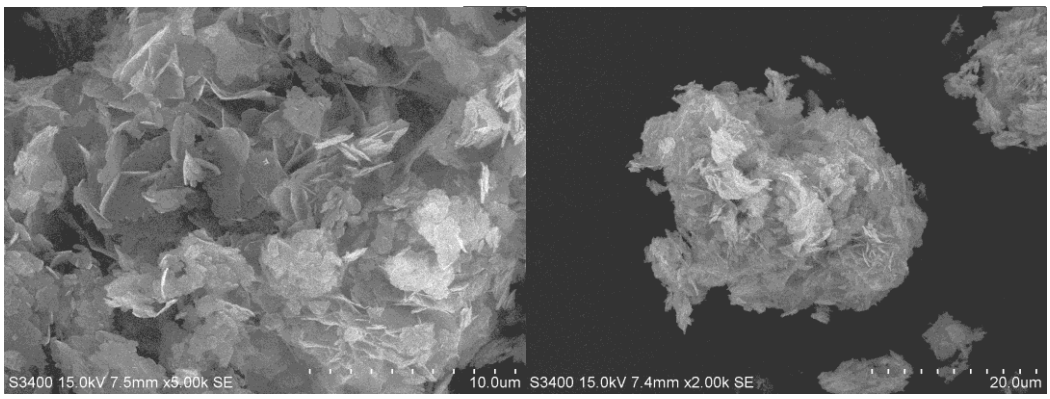

(e)

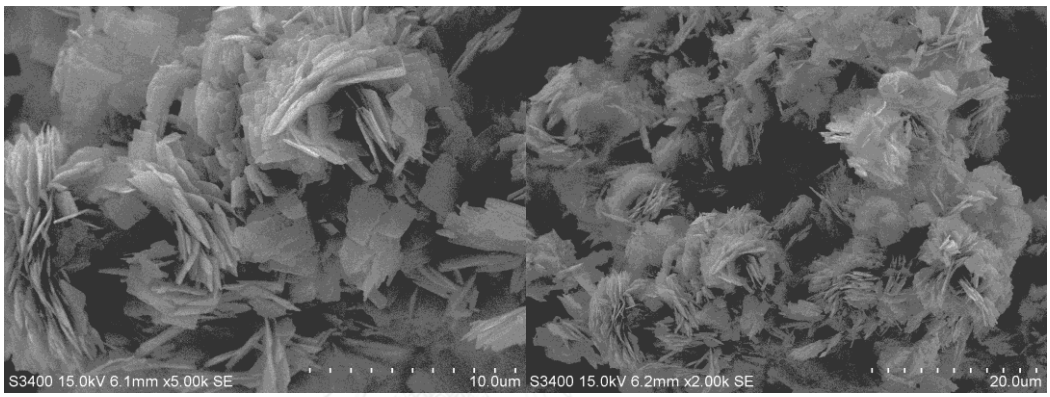

Figure 5.2 (cont.) SEM micrographs for (d) FeV and (e) MnV catalyst**;** When (i) ×5000 (ii) ×2000

The BiV catalyst had a thinner sheet and higher surface area than CoV catalyst. It also showed smaller size as compared with the unpromoted catalyst. Figure 5.1 (d) and (e) show SEM micrographs of Fe and Mn promoted catalysts, respectively. The catalyst structure of Fe and Mn doped VPO showed different sizes and shapes of crystal plates. The MnV catalyst formed rich rosette clusters with slightly smaller particle sizes, compared to the undoped catalyst but it showed larger clusters size as compared with FeV and the other metal-promoted catalysts. Some of the crystal plates of MnV were agglomerated resulting in the lower surface area [18]. The mentioned property such as small crystallite size, high surface area, and rich rosette clusters could give a great impact to selectivity and activity of the VPO catalyst.

5.4 Temperature program reduction (H_2-TPR)

The TPR profiles are presented by the TCD signals as a function of temperature as shown in Figure 5.3. The oxygen atoms removed were evaluated from the total area under the TPR profiles and the results are shown in Table 5.3. According to Mahdavi et al. [31], the reduction peak for VPO unpromoted catalysts were found at 622°C and 771°C. The first reduction peak, at low temperature about 622°C, was assigned to the removal of oxygen species that was V^{5+}-O^{2-} and the removal of the second peak at higher temperature (range from 700°C to 877°C) was the removed of the oxygen species associated with $V4^{+}$-O^{-}. Additionally, the two reduction peaks for VPO catalyst were shifted to the right as the effect of calcination temperature and holding time. The different types of V presented in each phase was in accordance with the existence of the V^{5+} and/or V^{4+} in the vanadium phosphates, in addition to the main phase of $VOPO_4$ and $(VO)_2P_2O_7$ phase, according to those previously reported [16, 32].

From many researches, $(VO)_2P_2O_7$ phase was reduced at high temperature around 844°C but it was over a limit of the laboratory instrument [31, 33]. In the H_2-TPR profiles of CoV, BiV, FeV, and MnV catalysts, the reducibility of V^{5+} was found at 596, 595, 591, and 569°C, respectively while the reducibility of V^{4+} was found at 765, 764, 803, and 725°C, respectively. The total amounts of oxygen atoms removal of unpromoted VPO, CoV, BiV, FeV, and MnV catalysts were calculated to be 2.93, 5.87, 3.98, 5.13, and 6.24 $\mathbf{x}10^{21}$ atoms/g catalyst, respectively.

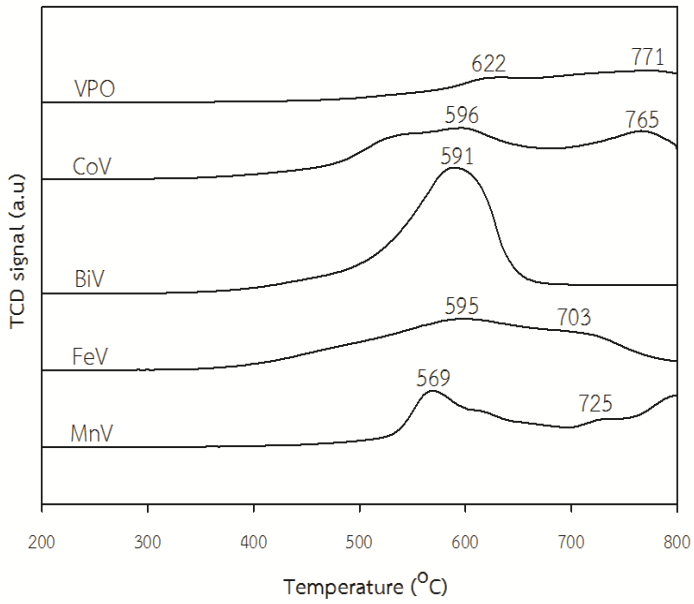

Figure 5.3 TPR in H_2 profiles of VPO undoped and doped catalysts

Table 5.3 Amounts of oxygen atoms removed obtained by H_2-TPR analyses for VPO undoped and doped catalysts

Catalyst	T_{max} (°C)	Oxygen atoms removed ($x10^{-3}$ mol/g)	Oxygen atoms removed ($x10^{21}$ atom/g)
VPO	622	1.77	1.06
	771	3.11	1.87
Total		4.88	2.93
CoV	596	5.41	3.25
	765	4.34	2.62
ToTal		9.75	5.87
BiV	591	6.61	3.98
	-	-	-
Total		6.61	3.98
FeV	595	4.22	2.54
	703	4.30	2.59
Total		8.52	5.13
MnV	569	4.81	2.91
	725	5.53	3.33
Total		10.35	6.24

The CoV catalyst exhibited higher oxygen atoms removal of V^{5+}, which enhanced a higher PA selectivity than the other promoted catalysts [5, 33]. The best correlation was reported between the amounts of oxygen removed from both V^{4+} and V^{5+} state, with the selectivity and activity of catalyst. From the TPR profiles, it can be estimated that the unpromoted VPO catalyst would give lower catalytic performance because it had lower total oxygen atoms removed as compared with the promoted catalyst. And the activity and selectivity of MnV catalyst in the partial oxidation of n-pentane would be higher than the other catalysts due to the highest amount of oxygen removal. In other words, it exhibited a higher removal of V^{4+} state.

5.5 X-ray photoelectron spectroscopy (XPS)

The oxidation state of V 2p, O 1s, Co 2p, Bi 4f, Fe 2p, and Mn 2p were investigated by using XPS technique. For the V 2p, each spectrum exhibited two peaks which are the characteristics of the structure of vanadium V $2p_{3/2}$ and V $2\,p_{1/2}$, corresponding to a spin orbital with specific binding energies. The binding energies 516.2-5165 eV correspond to V $2p_{3/2}$ (V^{4+} oxidation state) and the position binding energy at 517.3-517.7 eV correspond to V $2p_{3/2}$ (V^{5+} oxidation state) [34]. Another component in V 2p signals was attributed to V $2p_{1/2}$ (V^{4+} oxidation state) at 523.4 eV [4, 35]. Moreover, the values of binding energies suggesting V_2O_3 species with a V^{3+} oxidation state were detected at 515.3 and 522.8 eV, corresponding to $2p_{3/2}$ and $2p_{1/2}$, respectively.

The XPS binding energy (BE) of V 2p and O 1s for the unpromoted VPO and promoted catalysts are shown in Figure 5.4. The binding energies of V^{4+} species of VPO unpromoted, CoV, BiV, FeV, and MnV promoted catalyst were demonstrated at 517.5, 518.2, 518.5, 518.9, and 518.4 eV, respectively, and the V^{5+} species were presented at 518.8, 519.1, 519.7, 519.9, and 519.3 eV, respectively. Nevertheless, the binding energy of V $2p_{3/2}$ in this research was found to slightly shift to higher binding energy. This was because the electron density nearby vanadium atoms was decreased from an interaction between vanadium and metal doping component. This resulted in the increase the electron density of vanadium atom but decreased the electron density on metal atoms [36, 37].

The percentages of peak areas for V^{4+} and V^{5+} were calculated using the deconvolution of V $2p_{3/2}$ peaks that are evaluated in table 5.4. In the case of the Mn doped catalyst, the relative amount of the two oxidation species were V^{4+} 62.4%, V^{5+} 37.6%. The relative amounts of V^{4+} and V^{5+} in the VPO catalyst were 61.8% and 38.2%, respectively. It was found that the addition of transition metal into V_2O_5 resulted in a decrease in the vanadium oxidation state from V^{5+} to V^{4+}.

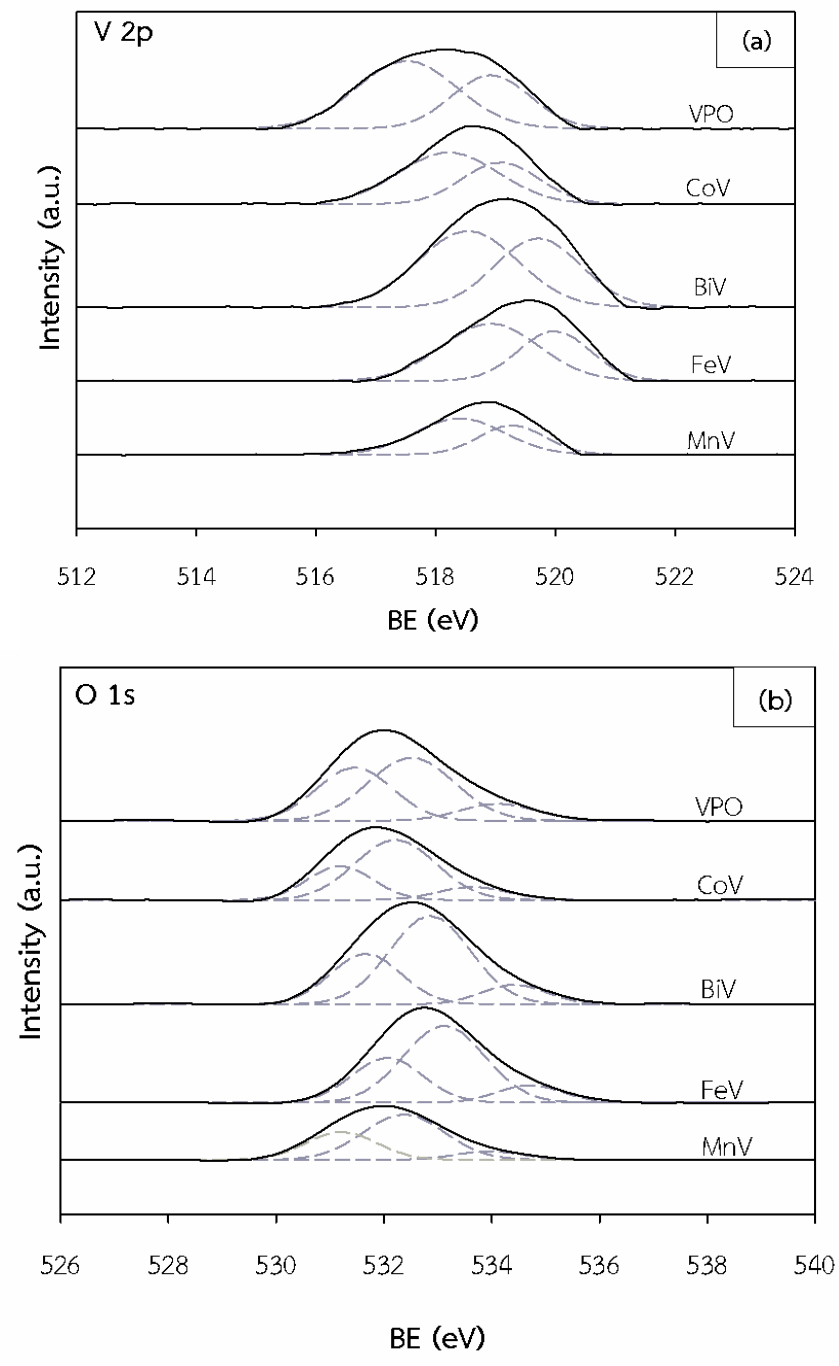

Figure 5.4 XPS spectra of (a) V 2p and (b) O 1s for VPO undoped, CoV, BiV FeV, and MnV doped catalysts

Table 5.4 XPS binding energies and distribution of oxidation state of VPO and transition metal promoted catalyst

Catalyst	Binding energies (eV)				%V^{4+}	%V^{5+}	V^{5+}/V^{4+}	%O_l**
	V^{4+}	V^{5+}	O_l*	O_s**				
VPO	517.5	518.8	531.5	532.5	61.8	38.2	0.62	42.5
CoV	518.2	519.1	531.2	532.2	61.7	38.3	0.62	34.8
BiV	518.5	519.7	531.5	532.8	56.4	43.6	0.77	33.2
FeV	518.9	519.9	532.0	533.1	60.9	39.1	0.64	33.6
MnV	518.4	519.3	531.2	532.4	62.4	37.6	0.60	31.1

* O_l was the lattice oxygen

**O_s was the surface oxygen

The O 1s XPS spectra for the unpromoted and the transition metal promoted catalysts were deconvoluted into three main peaks, as shown in Figure 5.4 (b). According to Amri et al. [43], the binding energy at 528.9-529.3 eV could be attributed to the lattice oxygen or O^{2-} and the binding energies around 530.9-531.3 eV were described as the surface oxygen from a wide variation of species such as adsorbed oxygen O^- and/or OH- species. The third peak of O 1s at higher binding energy was exhibited as the chemisorbed water about 532.1-532.4 eV [43, 44]. The amounts of %O_l of VPO unpromoted, CoV, BiV, FeV, and MnV promoted catalyst were evaluated in Table 5.4. The active oxygen species was studied by Abon et al. [45] and Taufiq-Yap et al. [46], they found that lattice oxygen was incorporated into the products.

5.6. Partial oxidation of n-pentane

The catalytic performances of all the samples in part I are illustrated in Figure 5.5, in terms of n-pentane conversion and selectivity of each product for unpromoted VPO and transition metal promoted catalysts. The increase of n-pentane conversion of the transition metals promoted V_2O_5 could be correlated to the increased number of active sites and the increase of activity with respect to metal dispersion on the surface of vanadium component. The vanadium and oxygen species had a direct relationship with n-pentane conversion. Moreover, the metal doped catalysts had an increased $(VO)_2P_2O_7$ phase according to the XRD patterns. Two dimensions illustration of SEM images also presented the rosette cultures. The catalyst, with thin plates and rich rosette shape have shown better catalytic performances in n-pentane oxidation [12, 20].

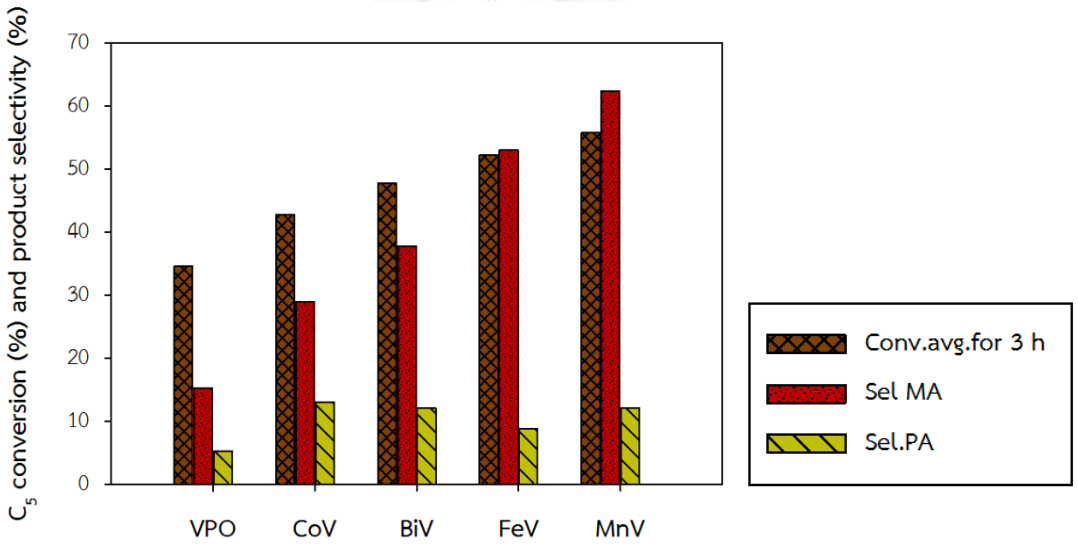

Figure 5.5 Chart of catalytic performances for VPO unpromoted and transition metal promoted catalysts

Among the catalysts studied, the MnV was found to exhibit the highest pentane conversion at 55.8%, followed by FeV, BiV, and CoV at 52.3%, 47.8%, and 42.7%, respectively. The differences in conversion for the promoted catalysts compared to the unpromoted catalyst were attributed to the reactivity of the oxygen atoms in lattice. Table 5.4 shows the average selectivity of MA, PA, and CO_2 at 3 h. The Mn doped (MnV) showed the maximum selectivity of MA and PA, at 62.5% and 12.1%, respectively. The MA selectivity of FeV, BiV, CoV, and VPO catalysts appeared at about 53.0, 37.8, 28.9, and 15.2 %, rescectively with PA selectivity 8.9%, 12.1%, 13.1%, and

5.3%, respectively. The addition of Mn into the VPO catalyst gave the highest MA and PA selectivity due to the higher specific surface area, smaller crystallite, and higher amount of oxygen species removed associated with V^{4+}. In other words, the conversion and selectivity of unpromoted were lower due to the higher amount of oxygen species associated with V^{5+} and bigger crystallite size.

Table 5.5 Evaluation of n-pentane conversion and productivity for unpromoted and promoted catalyst

Catalyst	n-Pentane conversion (%)	Liquid product sel.* (%)		
		MA	PA	By-product
VPO	34.6	15.2	5.3	79.5
CoV	42.7	28.9	13.1	58.0
BiV	47.8	37.8	12.1	50.1
FeV	52.3	53.0	8.9	38.1
MnV	55.8	62.5	12.1	25.4

* Average 3h

Part II

Comparison of the catalyst activities of the Mn-promoted VPO catalysts with different Mn/V ratios

The addition of Mn into the V_2O_5 catalysts improved the catalytic activity of the VPO due to higher surface area, smaller crystallite size, richer rosette shape morphologies, higher V^{4+} species, and higher oxygen atoms removed than the other catalysts as shown by the results in chapter 5 part I. The Mn promoted catalysts were then produced with different concentrations of Mn added, at 0.25, 0.35, 0.45, 0.55, and 0.65 mass ratio, and were denoted as 0.25MnV, 0.35MnV, 0.45MnV, 0.55MnV, and 0.65MnV, respectively. The effect of different concentrations of Mn on the physicochemical properties, reactivity and catalytic properties of the catalysts were investigated in part II.

5.7. XRD

Six characteristic peaks of $(VO)_2P_2O_7$ at 2θ = 22.9, 28.4, 33.8, 43.2, and 58.4^o which corresponded to (0 2 0), (2 0 4), (1 0 6), (0 0 8), and (3 1 9) planes, are shown in Figure 5.6. However, additional small peaks at 2θ = 21.5 and 24.3^o, which corresponded to δ-$VOPO_4$ phase and XRD peaks at 19.5 and 22.0^o corresponded to β-$VOPO_4$ phase were detected for all the Mn-doped VPO catalysts. This reflected the crystallite size of the catalysts that was increasing as the concentration of Mn promoter increased. Meanwhile, for the 0.45MnV catalyst the characteristic peaks at 2θ = 15.6 and 20.0^o were emerged and were attributed to the $VOHPO_4 \bullet 0.5H_2O$ and the peaks at 2θ = 26.1 and 29.1^o corresponded to α-$VOPO_4$, respectively [23, 47]. All the vanadium species were found in a V^{5+} state. Pierini et al. [48] reported structure and properties of metal promoted on VPO catalyst. They indicated that Mn dopant would favor the appearance of V^{5+} containing phases. However, the amount of Mn promoter added at higher mass ratios at 0.45, 0.55, and 0.65 resulted in the decreasing of V^{5+} phase intensity. Previous studies had proposed the effect of crystallite size of V^{5+} phase to be inversely proportional to the activity of the VPO catalysts. The smaller crystallite size contributed to higher active phase for the partial oxidation of n-pentane to MA and PA [6, 17].

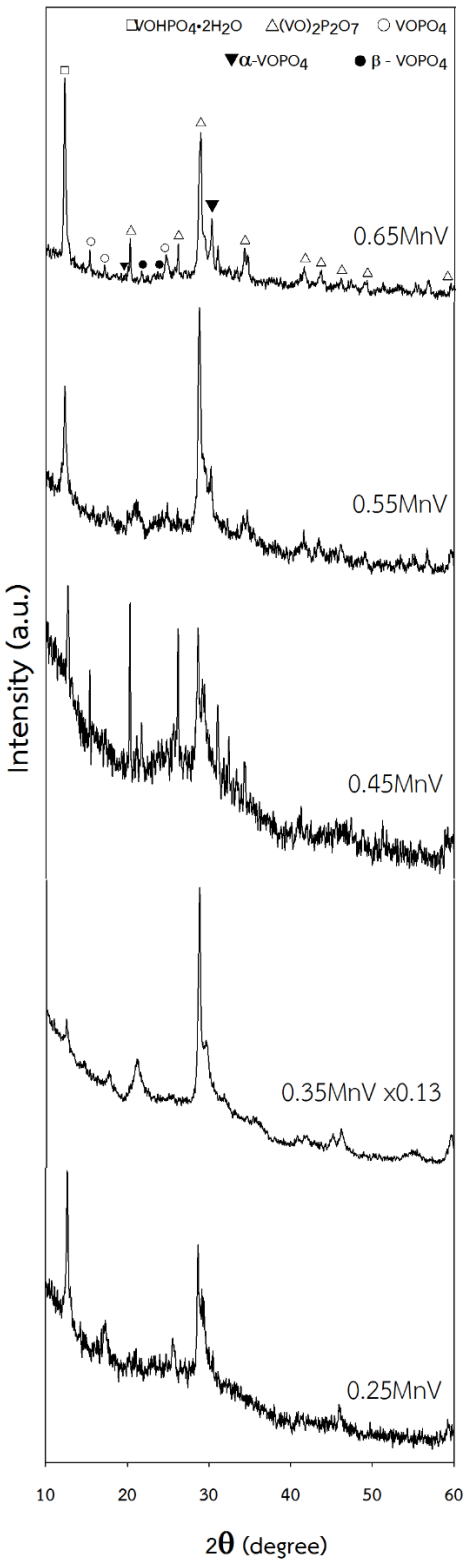

Figure 5.6 XRD patterns of catalyst with difference concentration of Mn as 0.25MnV, 0.35MnV, 0.45MnV, 0.55MnV, and 0.65MnV catalyst

5.8. Specific surface area and metals elemental measurements

The specific surface areas, pore volume, and average pore diameter of the MnV catalysts with different Mn/V ratios are presented in Table 5.5. The amount of BET surface area of 0.25MnV, 0.35mnV, 0.45MnV, 0.55MnV, and 0.65MnV catalyst were evaluated 7.3, 10.16, 8.3, 12.9, and 8.9m²/g, respectively. The average pore diameter depended on the concentration of Mn promotion. The average pore diameter and crystallite size decreased with increasing Mn loading. Surface area of the 0.25MnV catalyst was reduced to 7.3m^2/g as compared with surface area of the 0.35MnV catalyst (10.2m^2/g). The specific surface areas were gradually decreased as the Mn promoter increased from 0.35 to 0.65 ratios into VPO component. It is indicated that Mn components were dispersed onto VPO surface. Moreover, the dispersion of Mn resulted in the reduction of the average pore size from 16.4 to 9.6 nm (Table 5.5) [45, 46].

Table 5.6 Specific surface areas, pore volume, and average pore diameter present in 0.25MnV, 0.35MnV, 0.45MnV, 0.55MnV, and 0.65MnV catalyst

Catalyst	N_2 physisorption results		
	BET surface area (m²/g)	Pore volume (x10^{-1}cm³/g)	Average pore diameter (nm)
0.25MnV	7.3	0.19	16.4
0.35MnV	10.16	0.26	13.1
0.45MnV	8.3	0.15	12.4
0.55MnV	12.9	0.38	9.6
0.65MnV	8.9	0.24	11.3

5.9. SEM-EDX

EDX was used to analyze the elemental compositions of the Mn promoted catalysts and the results are shown in Table 5.6. The M/V ratios from EDX analysis for 0.25MnV, 0.35MnV, 0.45MnV, 0.55MnV, and 0.65MnV catalyst were 0.25, 0.26, 0.42, 0.50, and 0.69, respectively. The weight percents of V, P, and Mn are given in Table 5.6 without the weigh percent of O composition. Nie et al. [45] explain that the degree of P enrichment became more pronounced at higher Mn loading. This was due to the effect of high Mn loading interaction onto the VPO phase, so tendency of P in the catalysts increased as the amounts of metal loading increased [45].

Table 5.7 Chemical compositions of 0.25MnV, 0.35MnV, 0.45MnV, 0.55MnV, and 0.65MnV catalyst

Catalyst	EDX analyzed (wt%)			Mass Ratio of EDX	
	V	P	M*	P/V	M/V
0.25MnV	48.3	39.6	12.1	0.81	0.25
0.35MnV	48.6	38.8	12.6	0.79	0.26
0.45MnV	43.9	37.6	18.5	0.86	0.42
0.55MnV	26.3	26.1	13.2	0.99	0.50
0.65MnV	25.9	24.4	17.9	0.94	0.69

* M was Mn promoter

The effect of Mn loading on the morphology of the vanadyl pyrophosphate catalysts is illustrated by SEM micrographs in Figure 5.7. The present of 0.25 Mn/V ratios in Figure 5.7 (a) showed the structure of crystalline plates of $(VO)_2P_2O_7$ that started to form and agglomerate into rosette shape cluster but uncompleted rose clusters. Moreover, the rosette shape cluster became more obvious and larger at 0.35 and 0.45 ratios (Figure 5.7 (b) and (c)). The layers of rosette shape were illustrious to increase the exposure of $(VO)_2P_2O_7$ phase [12, 27, 29]. The results from XRD and SEM analyses revealed that increasing the amount of Mn loading promoted agglomeration of the VPO platelets into rosette forms. However, as can be seen from Figure 5.7 (d) and (e), the rosette plates were flattened and less spitted. It was believed that the $(VO)_2P_2O_7$ phase was changed to the $VOPO_4$ phase. Moreover, the higher amount of Mn inhibited the growing of rosette shape.

.

(a)

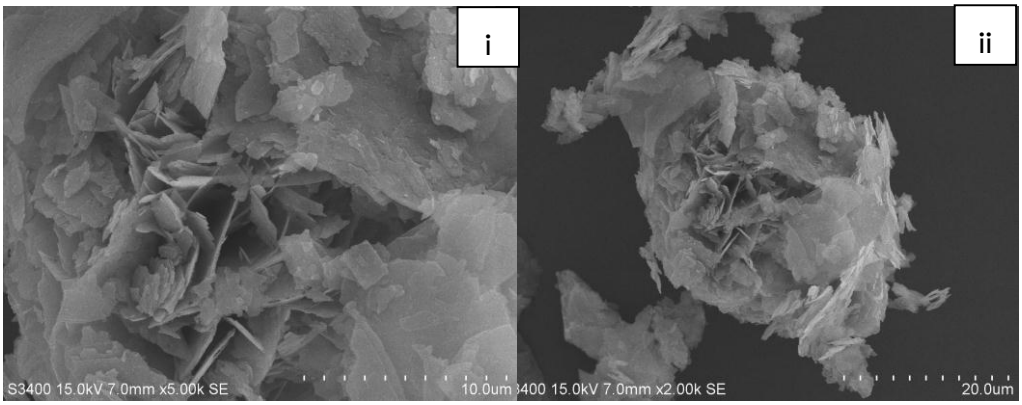

(b)

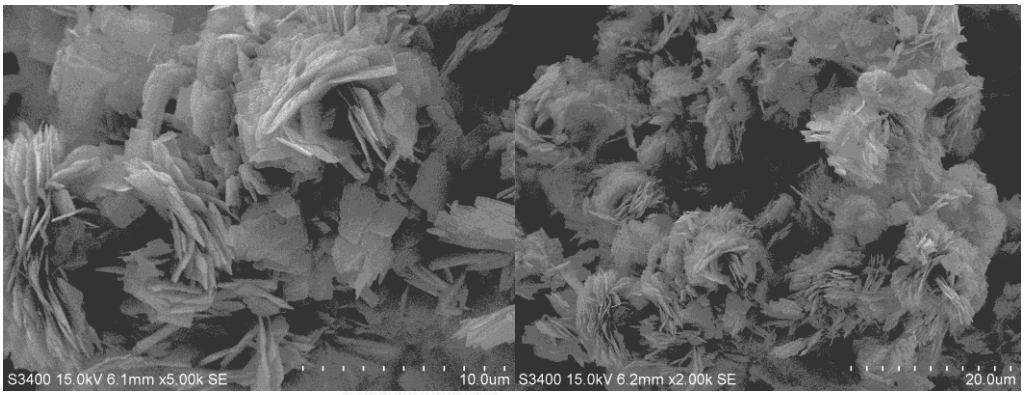

(c)

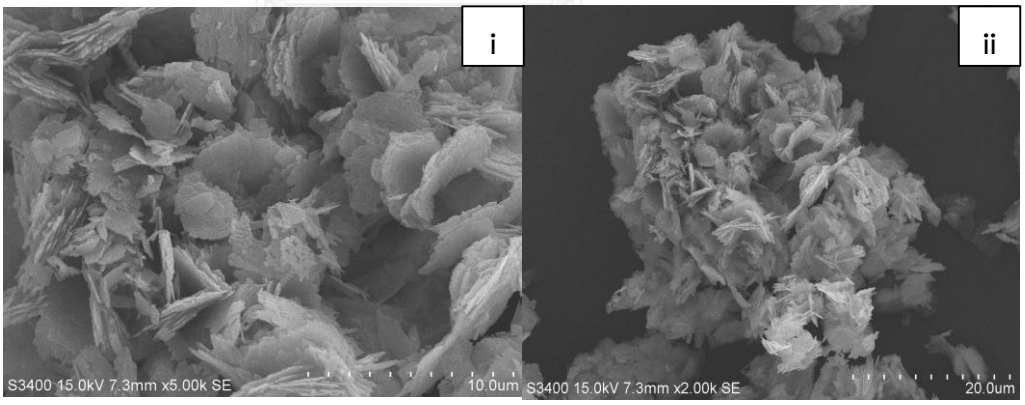

Figure 5.7 SEM micrographs for (a) 0.25MnV (b) 0.35MnV catalyst, and (c) 0.45MnV; When (i) ×5000 (ii) ×2000

(d)

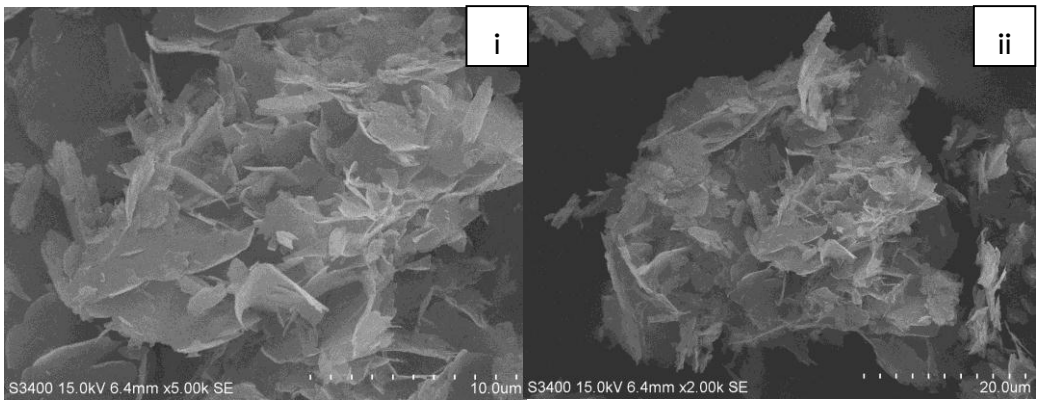

(e)

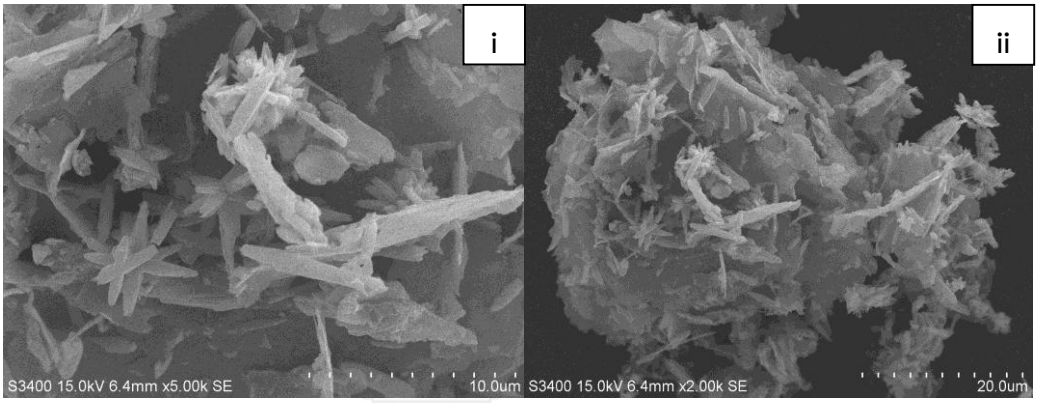

Figure 5.7 (cont.) SEM micrographs for (d) 0.55MnV, and (e) 0.65MnV catalyst**;** When (i) ×5000 (ii) ×2000

5.10. H_2-TPR

The nature of the oxidizing species, which directly affects the reduction property of catalysts, could lead to a great impact on the catalytic activity and selectivity. Thus, it was important to determine the kinds of oxygen species available in the catalysts [18, 31]. The H_2 TPR profiles are shown in Figure 5.8 and Table 5.6 reports the amounts of removed oxygen in each peak. The Mn promoted V_2O_5 catalysts showed two reduction peaks in the range of 537 to 600 ^oC (low reduction temperature) and from 700 to 765 ^oC which ascribes as high reduction temperature. Both reduction peaks were specified to the removal of oxygen species from V^{5+}-O^{2-} and V^{4+}-O^- state, respectively [16, 33]. The amounts of removal of both V^{5+}-O^{2-} and V^{4+}-O^- were found to increase with increasing amount of Mn loading. The 0.25MnV catalyst gave characteristics of two reduction peaks at 537 and 707^oC and the amount of oxygen removed from each peak were 2.1 x 10^{21} and 3.3 x 10^{21} atoms/g, respectively. The 0.35MnV, 0.45MnV, 0.55MnV, and 0.65MnV catalysts gave similar reduction peaks as those of 0.25MnV catalyst. The first peak occurred at higher temperature ~725^oC and the amounts of oxygen removed were 3.3 x 10^{21}, 4.1 x 10^{21}, 2.4 x 10^{21}, and 1.9 x 10^{21}, respectively. The second peak occurred at lower temperature ~560^oC and the amounts of oxygen removed were 2.9 x 10^{21}, 2.8 x 10^{21}, 1.7 x 10^{21}, and 1.4 x 10^{21}, respectively. However, the 0.45MnV catalyst showed a markedly increment for the reduction of V^{4+}, which could initiate a better performances of the catalyst compared to the other catalysts [16, 21, 47]. However, at higher Mn ratios loading the amounts of oxygen removed were decreased suggesting a strong interaction between manganese and oxygen.

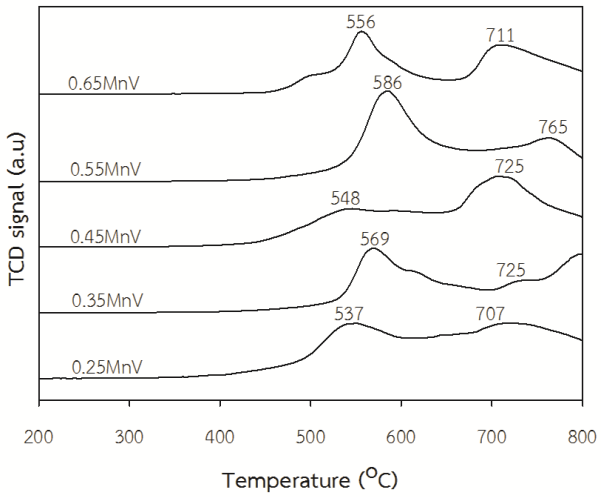

Figure 5.8 TPR in H_2 profiles of difference Mn loading catalysts

Table 5.8 Amounts of oxygen atoms removed obtained by H_2-TPR analyses for difference Mn loading catalysts.

Catalyst	T_{max} (°C)	Oxygen atoms removed ($x10^{-3}$ mol/g)	Oxygen atoms removed ($x10^{21}$ atom/g)
0.25MnV	584	3.4	2.1
	725	5.4	3.3
Total		**8.8**	**5.4**
0.35MV	569	4.8	2.9
	725	5.5	3.3
ToTal		**10.2**	**6.2**
0.45MnV	537	4.7	2.8
	707	6.7	4.1
Total		**11.4**	**6.9**
0.55MnV	586	2.8	1.7
	765	4.0	2.4
Total		**6.8**	**4.1**
0.65MnV	556	2.4	1.4
	711	3.2	1.9
Total		**5.6**	**3.3**

5.11. XPS

The oxidation number of vanadium and the composition of V^{5+} and V^{4+} oxidation states on the MnV catalysts are evaluated in Table 5.7. The V $2p_{3/2}$ and O 1s were deconvorluted as shown in Figure 5.9. The binding energies of V^{4+} states of 0.25MnV, 0.35MnV, 0.45MnV, 0.55MnV, and 0.65MnV catalysts were demonstrated at 517.6, 518.4, 518.8, 519.8, and 518.3 eV, respectively and the V^{5+} states were presented at 518.6, 519.3, 519.9, 520.5, and 519.6 eV, respectively. The binding energys of V $2p_{3/2}$ were found to slightly shift to higher binding energy because of an intimate contact between vanadium and manganese component. The increase of the electron density of vanadium atoms produced decreased electron density of manganese atoms [36, 37].

In the case of the 0.25MnV, 0.35MnV, 0.45MnV, 0.55MnV, and 0.65MnV catalysts, the relative amount of the V^{4+} oxidation state species were 41.7%, 62.4%, 65.1%, 47.1%, and 43.6%, respectively. The 0.45MnV catalyst precented the best catalytic performances because it gave a higher amount of V^{4+} that was consistent with the results from XRD, SEM-EDX, and H_2-TPR analysis.

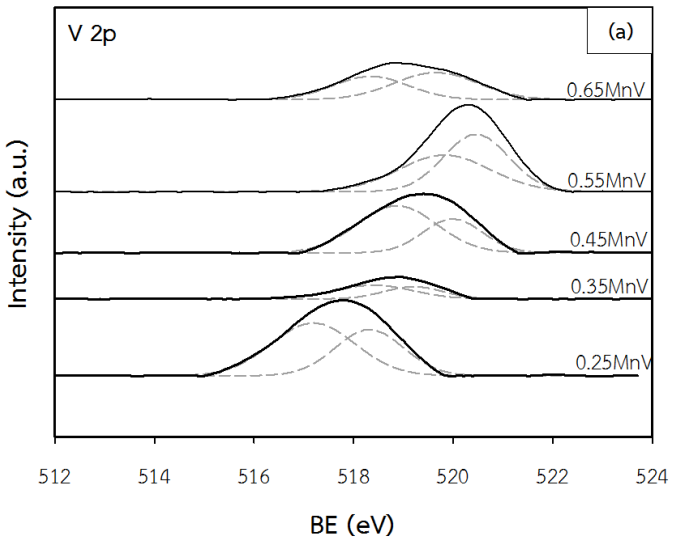

Figure 5.9 XPS spectra of (a) V 2p and (b) O 1s for 0.25MnV, 0.35MnV, 0.45MnV, 0.55MnV, and 0.65MnV catalysts

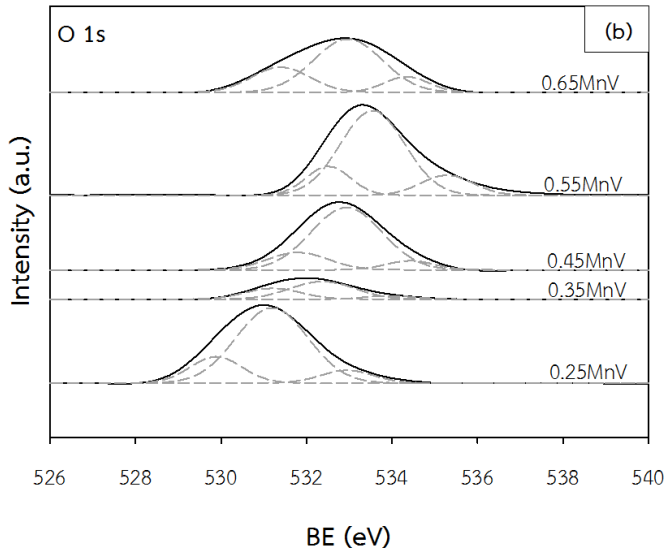

Figure 5.9 (cont.) XPS spectra of (a) V 2p and (b) O 1s for 0.25MnV, 0.35MnV, 0.45MnV, 0.55MnV, and 0.65MnV catalysts

Table 5.9 XPS binding energies and distribution of oxidation state for 0.25MnV, 0.35MnV, 0.45MnV, 0.55MnV, and 0.65MnV catalysts

Catalyst	Binding energies (eV)				%V^{4+}	%V^{5+}	%O_l**
	V^{4+}	V^{5+}	O_l*	O_s**			
0.25MnV	518.4	519.6	531.2	532.5	41.7	58.3	20.2
0.35MnV	518.4	519.3	531.2	532.4	62.4	37.6	31.1
0.45MnV	518.8	519.9	531.8	532.0	65.1	34.9	20.0
0.55MnV	519.8	520.5	532.5	533.5	47.1	52.9	19.0
0.65MnV	518.3	519.6	531.3	532.3	43.6	56.4	28.6

* O_l was the lattice oxygen

**O_s was the surface oxygen

5.12. Catalytic testing

The catalytic performances of the different Mn loading catalysts were tested in the partial oxidation of n-pentane to Ma and PA at 400°C (GHSV 3050 h^{-1}). The catalytic activity in terms of pentane conversion and selectivity of MA and PA are presented in Figure 5.10 and Table 5.8. The 0.45MnV catalyst provided the highest n-pentane conversion and selectivity of MA and PA at 57.9%, 66.2% and 6.12%, respectively, as compared to the other catalysts studied. The rich rosette shape layer of the catalyst could provide accessibility of the reactant onto the active surface of catalyst [15, 47]. The MA selectivity for 0.25MnV, 0.35MnV, 0.55MnV, and 0.65MnV catalysts were 38.2%, 62.5%, 42.6%, and 33.1%, respectively and PA selectivity were 8.54%, 12.1%, 2.2%, and 5.4%, respectively. The selectivity of MA was increased as the amount of Mn doping increased except 0.55MnV and 0.65MnV catalysts. The lower MA selectivity at higher amounts of Mn concentration may be due to the increasing amount of V^{5+} species as revealed by the results from XRD analysis [18, 47]. In addition, the results from SEM analysis showed the rosette plates that were flattened and less splited for these catalyst compositions. As aconsequence, the MA and PA selectivity were inhibited. The n-pentane conversion for 0.25MnV, 0.35MnV, 0.55MnV, and 0.65MnV catalysts were 45.0%, 55.8%, 52.6%, and 52.9%, respectively.

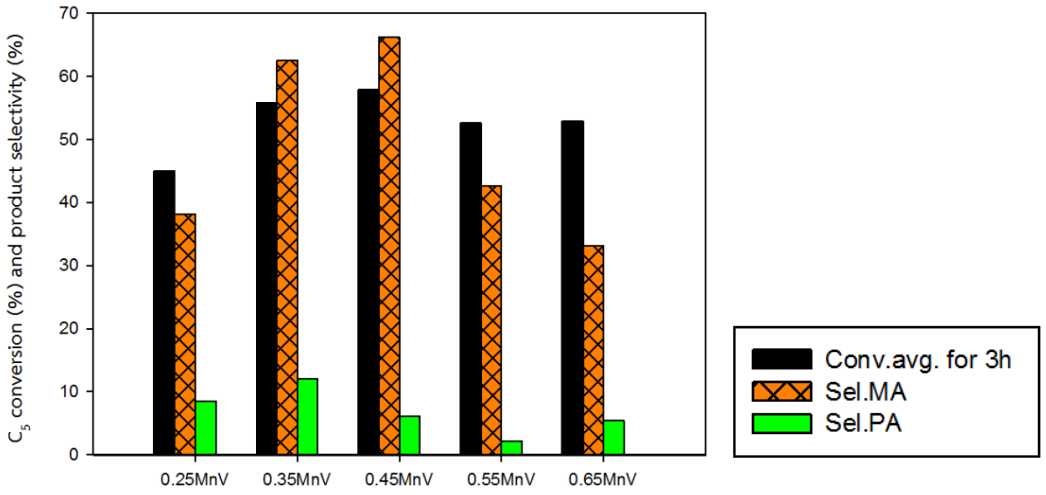

Figure 5.10 Chart of catalytic performances for difference Mn loading catalysts

Table 5.10 Evaluation of n-pentane conversion and productivity for difference Mn loading catalysts

Catalyst	n-Pentane conversion (%)	Liquid product sel.* (%)		
		MA	PA	By-product
0.25MnV	45.0	38.2	8.5	53.3
0.35MnV	55.8	62.5	12.1	25.4
0.45MnV	57.9	66.2	6.1	27.7
0.55MnV	52.6	42.6	2.2	55.2
0.65MnV	52.9	33.1	5.4	61.5

* Average 3h

CHAPTER 6
CONCLUSIONS

6.1 Conclusions

6.1.1. Among the different metals (M = Co, Bi, Fe, and Mn) doped VPO catalysts with M/V mass ratio 0.35, the Mn doped catalyst showed the best catalytic performances in n-pentane partial oxidation in terms of both MA and PA selectivity and n-pentane conversion. The presence of Mn may enhance the re-oxidation of catalyst. The catalyst performances were correlated to the amount of V^{4+} species, the higher amount of $(VO)_2P_2O_7$ phase, smaller crystallite, rich rosette shape morphologies, higher specific surface area, and higher amount of oxygen species removed from V^{4+}-O^-.

6.1.2. For the Mn promoted VPO catalysts, the optimized Mn loading (M/V mass ratio) was determined to be at 0.45. It provided the highest n-pentane conversion at 57.9% with the selectivity of MA and PA 66.2% and 6.1%, respectively. Further increase of the amount of Mn doping to 0.55MnV and 0.65MnV led to lower selectivity of MA due probably to the increased amount of V^{5+} state and that the rosette-plates morphologies were flattened, and also low oxygen atoms removal.

6.2 Recommendation

6.2.1. Further study on the effect of different calcination temperatures on the physico-chemical, reactivity and catalytic properties of VPO catalysts should be investigated.

6.2.2. The effect of different supports such as Al_2O_3 and SiO_2 should be considered in the future study.

REFERENCES

[1] Singh, S. Partial oxidation of n-pentane over vanadium phosphorus oxide supported on hydroxyapatites. South African Journal of Chemistry 69 (2016): 1-8.

[2] Dmuchovsky, B., Freerks, M.C., Pierron, E.D., Munch, R.H., and Zienty, F.B. A study of the catalytic oxidation of benzene to maleic anhydride. Journal of Catalysis 4(2) (1965): 291-300.

[3] deMilt, C. Auguste Laurent, Founder of Modern Organic Chemistry. Chymia 4 (1953): 85-114.

[4] Schacht, L., Navarrete, J., Schacht, P., and Ramírez, M.A. Influence of vanadium oxidation states on the performance of V-Mg-Al mixed-oxide catalysts for the oxidative dehydrogenation of propane. Journal of the Mexican Chemical Society 54(2) (2010): 69-73.

[5] Bignardi, G., et al. Influence of the oxidation state of vanadium on the reactivity of V/P/O, catalyst for the oxidation of n-pentane to maleic and phthalic anhydrides. Journal of Molecular Catalysis A: Chemical 244(1) (2006): 244-251.

[6] Cavani, F., Colombo, A., Trifiro, F., Sananes Schulz, M., Volta, J., and Hutchings, G. The effect of cobalt and iron dopants on the catalytic behavior of V/P/O catalysts in the selective oxidation of n-pentane to maleic and phthalic anhydrides. Catalysis letters 43(3) (1997): 241-247.

[7] Cleaves, J. and Centi, G. The reaction mechanism of alkane selective oxidation on vanadyl pyrophosphate catalysts. Features gleaned from TAP reactor transient response studies. Catalysis today 16(1) (1993): 69-78.

[8] Chen, B. and Munson, E.J. Investigation of the mechanism of n-butane oxidation on vanadium phosphorus oxide catalysts: evidence from isotopic labeling studies. Journal of the American Chemical Society 124(8) (2002): 1638-1652.

[9] Zimmerman, W.H., Rossin, J.A., and Bukur, D.B. Effect of particle size on the activity of a fused iron Fischer-Tropsch catalyst. Industrial & engineering chemistry research 28(4) (1989): 406-413.

[10] Loehr, T., Martell, A., and Sawyer, D. Oxygen Complexes and Oxygen Activation by Transition Metals. 1988, Plenum, New York.

[11] Coulston, G.W., et al. The kinetic significance of V5+ in n-butane oxidation catalyzed by vanadium phosphates. Science 275(5297) (1997): 191-193.

[12] Xuan, Z.-Q. Gas-phase selective oxidation of C3-C4 hydrocarbon using only molecular oxygen. Ann Arbor 1050 (2009): 48106-1346.

[13] Smith, J. and Hergenrother, P. CHEMISTRY AND PROPERTIES OF PHENYLETHYNYL PHTHALIC-ANHYDRIDE IMIDE OLIGOMERS. in ABSTRACTS OF PAPERS OF THE AMERICAN CHEMICAL SOCIETY, pp. 23-POLY: AMER CHEMICAL SOC 1155 16TH ST, NW, WASHINGTON, DC 20036, 1994.

[14] Maccia, C.A., Bernstein, I.L., Emmett, E.A., and Brooks, S.M. In Vitro Demonstration of Specific IgE in Phthalic Anhydride Hypersensitivity 1–3. American review of respiratory disease 113(5) (1976): 701-704.

[15] Loh, P.X. Modified vanadium based oxide catalysts for selective oxidation of n-butane to maleic anhydride. UTAR, 2012.

[16] Schüth, F., Hesse, M., and Unger, K.K. Precipitation and coprecipitation. Handbook of heterogeneous catalysis (2008).

[17] Rownaghi, A.A., Taufiq-Yap, Y.H., and Rezaei, F. High surface area vanadium phosphate catalysts for n-butane oxidation. Industrial & engineering chemistry research 48(16) (2009): 7517-7528.

[18] Fan, X.-B., Dummer, N.F., Taylor, S.H., Bartley, J.K., and Hutchings, G.J. Preparation of vanadium phosphate catalyst precursors for the selective oxidation of butane using α, ω-alkanediols. Catalysis today 183(1) (2012): 52-57.

[19] Zazhigalov, V. Effect of Bismuth Additives on the Properties of Vanadium–Phosphorus Oxide Catalyst in the Partial Oxidation of n-Pentane. Kinetics and Catalysis 43(4) (2002): 514-521.

[20] Taufiq-Yap, Y., Kamiya, Y., and Tan, K. Promotional effect of bismuth as dopant in bi-doped vanadyl pyrophosphate catalysts for selective oxidation of n-butane to maleic anhydride. Journal of natural gas chemistry 15(4) (2006): 297-302.

[21] Goh, C.K., Taufiq-Yap, Y., Hutchings, G.J., Dummer, N., and Bartley, J. Influence of Bi–Fe additive on properties of vanadium phosphate catalysts for n-butane oxidation to maleic anhydride. Catalysis today 131(1) (2008): 408-412.

[22] de Farias, A.M.D., et al. Vanadium phosphorus oxide catalyst modified by niobium doping for mild oxidation of n-butane to maleic anhydride. Journal of Catalysis 208(1) (2002): 238-246.

[23] Taufiq-Yap, Y., Theam, K.L., Hutchings, G.J., Dummer, N., and Bartley, J.K. The Effect of Cr, Ni, Fe, and Mn Dopants on the Performance of Hydrothermal Synthesized Vanadium Phosphate Catalysts for n-Butane Oxidation. Petroleum Science and Technology 28(10) (2010): 997-1012.

[24] Cheburakova, E. and Zazhigalov, V. Reaction mechanism-based design of efficient VPO catalysts for n-C5H12 oxidation into phthalic, maleic, and citraconic anhydrides. Kinetics and Catalysis 49(4) (2008): 552-561.

[25] Taufiq-Yap, Y., Leong, L., and Irmawati, R. n-Butane Oxidation over γ-Al 2 O 3 Supported Vanadium Phosphate Catalysts. Journal of natural gas chemistry 16(3) (2007): 266-272.

[26] Taufiq-Yap, Y.H., Yuen, C.S., and Irmawati, R. Effects of Bi and Ni on the properties of a vanadium phosphorus oxide catalyst. Chinese Journal of Catalysis 35(2) (2014): 270-276.

[27] Carrara, C., Irusta, S., Lombardo, E., and Cornaglia, L. Study of the Co-VPO interaction in promoted n-butane oxidation catalysts. Applied Catalysis A: General 217(1) (2001): 275-286.

[28] Guliants, V., Benziger, J., Sundaresan, S., Wachs, I., and Hirt, A. Effect of promoters for n-butane oxidation to maleic anhydride over vanadium–phosphorus-oxide catalysts: comparison with supported vanadia catalysts. Catalysis letters 62(2-4) (1999): 87-91.

[29] Michalakos, P., Birkeland, K., and Kung, H.H. Selective oxidation of pentane over Al2O3-and SiO2-supported vanadia catalysts. Journal of Catalysis 158(1) (1996): 349-353.

[30] TAUFIQ-YAP, Y.H. and GHANI, A.A.A. Synthesis and characterization of Ni-doped vanadium phosphorus oxide catalysts. Chinese Journal of Catalysis 28(12) (2007): 1037-1040.

[31] Zazhigalov, V., et al. A novel route in partial oxidation ofn-pentane over the VPO catalysts: formation of citraconic anhydride. Catalysis letters 37(1-2) (1996): 95-99.

[32] Yamamoto, N., Hiyoshi, N., and Okuhara, T. Thin-Layered Sheets of VOHPO4⊙ 0.5 H2O Prepared from VOPO4⊙ 2H2O by Intercalation− Exfoliation− Reduction in Alcohol. Chemistry of materials 14(9) (2002): 3882-3888.

[33] Wong, Y.C. and Taufiq-Yap, Y. VOPO4· 2H2O and the vanadium phosphate catalyst produced by sonochemical synthesis. Asian Journal of Chemistry 23(9) (2011): 3853.
[34] Cornaglia, L., Carrara, C., Petunchi, J., and Lombardo, E. The role of cobalt as promoter of equilibrated vanadium–phosphorus–oxygen catalysts. Applied Catalysis A: General 183(1) (1999): 177-187.
[35] Taufiq-Yap, Y., Tan, K., Waugh, K.C., Hussein, M.Z., Ramli, I., and Abdul Rahman, M. Bismuth-modified vanadyl pyrophosphate catalysts. Catalysis letters 89(1) (2003): 87-93.
[36] Mahdavi, V. and Hasheminasab, H.R. Vanadium phosphorus oxide catalyst promoted by cobalt doping for mild oxidation of benzyl alcohol to benzaldehyde in the liquid phase. Applied Catalysis A: General 482 (2014): 189-197.
[37] Wang, C., Yang, S., Chang, H., Peng, Y., and Li, J. Structural effects of iron spinel oxides doped with Mn, Co, Ni and Zn on selective catalytic reduction of NO with NH 3. Journal of Molecular Catalysis A: Chemical 376 (2013): 13-21.
[38] Bautista, F., Campelo, J., Luna, D., Luque, J., Marinas, J., and Siles, M. Study of catalytic behaviour and deactivation of vanadyl-aluminum binary phosphates in selective oxidation of o-xylene. Chemical Engineering Journal 120(1) (2006): 3-9.
[39] Luciani, S., Cavani, F., Dal Santo, V., Dimitratos, N., Rossi, M., and Bianchi, C.L. The mechanism of surface doping in vanadyl pyrophosphate, catalyst for n-butane oxidation to maleic anhydride: The role of Au promoter. Catalysis today 169(1) (2011): 200-206.
[40] Silversmit, G., Depla, D., Poelman, H., Marin, G.B., and De Gryse, R. Determination of the V2p XPS binding energies for different vanadium oxidation states (V 5+ to V 0+). Journal of Electron Spectroscopy and Related Phenomena 135(2) (2004): 167-175.
[41] Shang, D., Zhong, Q., and Cai, W. High performance of NO oxidation over Ce–Co–Ti catalyst: The interaction between Ce and Co. Applied Surface Science 325 (2015): 211-216.
[42] Liu, W. and Flytzani-Stephanopoulos, M. Transition metal-promoted oxidation catalysis by fluorite oxides: A study of CO oxidation over Cu CeO2. The Chemical Engineering Journal and the Biochemical Engineering Journal 64(2) (1996): 283-294.
[43] Amri, A., Duan, X., Yin, C.-Y., Jiang, Z.-T., Rahman, M.M., and Pryor, T. Solar absorptance of copper–cobalt oxide thin film coatings with nano-size, grain-like morphology: optimization and synchrotron radiation XPS studies. Applied Surface Science 275 (2013): 127-135.
[44] Kan, J., et al. Performance of co-doped Mn-Ce catalysts supported on cordierite for low concentration chlorobenzene oxidation. Applied Catalysis A: General 530 (2017): 21-29.
[45] Abon, M., Bere, K., and Delichere, P. Nature of active oxygen in the n-butane selective oxidation over well-defined V P O catalysts: an oxygen isotopic labelling study. Catalysis today 33(1-3) (1997): 15-23.
[46] Taufiq-Yap, Y., Sakakini, B., and Waugh, K. On the mechanism of the selective oxidation of n-butane, but-1-ene and but-1, 3-diene to maleic anhydride over a vanadyl pyrophosphate catalyst. Catalysis letters 46(3) (1997): 273-277.
[47] Klose, B.S., Jentoft, F.C., Schlögl, R., Subbotina, I.R., and Kazansky, V.B. Effect of Mn and Fe on the reactivity of sulfated zirconia toward H2 and n-butane: a diffuse reflectance IR spectroscopic investigation. Langmuir 21(23) (2005): 10564-10572.
[48] Pierini, B.T. and Lombardo, E.A. Structure and properties of Cr promoted VPO catalysts. Materials chemistry and physics 92(1) (2005): 197-204.

[49] Nie, W., Wang, X., Ji, W., Yan, Q., Chen, Y., and Au, C. A study on VPO specimen supported on aluminum-containing MCM-41 for partial oxidation of n-butane to MA. Catalysis letters 76(3) (2001): 201-206.

[50] Nie, W., Wang, Z., Ji, W., Chen, Y., and Au, C. Comparative studies on the VPO specimen supported on mesoporous Al-containing MCM-41 and large-pore silica. Applied Catalysis A: General 244(2) (2003): 265-272.

[51] Taufiq-Yap, Y.H., Asrina, S.N., Hutchings, G.J., Dummer, N.F., and Bartley, J.K. Effect of tellurium promoter on vanadium phosphate catalyst for partial oxidation of n-butane. Journal of natural gas chemistry 20(6) (2011): 635-638.

APPENDIX

APPENDIX A

CALCULATION FOR CATALYST PREPARATION

Vanadium phosphorus oxide (VPO) catalysts were promoted with different transition metals (M = Co, Bi, Fe, and Mn) by precipitation method. The P/V and M/V mass ratios as 1.15 and 0.35 were shown below. In this research, 2 g of the V_2O_5 were used for all preparation and calculation based on 100 g of catalyst used.

A) Example calculation of CoV promoted catalyst

Molecular weight of any component:

V_2O_5	= 181.88 g/mol	$Co(NO_3)_3 \bullet 6H_2O$	= 97.97 g/mol
H_3PO_4	= 97.97 g/mol	Co	= 58.93 g/mol
V	= 50.94 g/mol	P	= 30.97 g/mol

A.1) V_2O_5 calculate

$$V = \frac{\text{weight of } V_2O_5 \times \text{molecular weight of V}}{\text{molecular weight of } V_2O_5}$$

$$V = \frac{2\ g \times 50.9\ g/mol}{181.88\ g/mol}$$

$\therefore$ V = 0.56 g

A.2) 1.15 P/V mass ratio

$$\text{Volume of } H_3PO_4 \text{ required} = \frac{\text{weight of P} \times \text{molecular weight of } H_3PO_4}{\text{molecular weight of P}}$$

$$H_3PO_4 = \frac{0.644\ g \times 97.97\ g/mol}{30.97\ g/mol}$$

H_3PO_4 = 2.04 g or H_3PO_4 = 1.08 ml

A.3) 0.35 Co/V mass ratio

$$\text{Weight of } Co(NO_3)_3 \bullet 6H_2O \text{ required} = \frac{\text{weight of Co} \times \text{MW of } Co(NO_3)_3 \bullet 6H_2O}{\text{MW of Co}}$$

$$\text{Weight of } Co(NO_3)_3 \cdot 6H_2O \text{ required} = \frac{0.196 \times 290.93}{58.93} = 0.97 \text{ g}$$

A.4) 0.25 Mn/V mass ratio

$$\text{Weight of } (CH_3COO)_2Mn \cdot 4H_2O \text{ required} = \frac{\text{weight of Mn} \times \text{MW of } (CH_3COO)_2Mn \cdot 4H_2O}{\text{MW of Mn}}$$

$$\text{Weight of } (CH_3COO)_2Mn \cdot 4H_2O \text{ required} = \frac{0.14 \times 245.09}{54.93} = 0.62 \text{ g}$$

APPENDIX B

CALCULATION OF AMOUNT OF OXIGEN SPECIES REMOVED FROM CATALYST THROUGH TPR IN H_2 ANALYSIS

Calcination the amount of oxygen atom removal by TPR in H_2 profile evaluate as follows:

B.1) Calculation the amount of oxygen removed for MnV catalyst

Amount of oxygen removed for AgO standard = 8.25×10^{-4} mol

Area of AgO reducing = 60.13

Amount of oxygen removed for MnV catalyst $\left(\frac{\text{mol}}{\text{g}}\right)$

$$= \frac{\text{Reducible area of MnV catalyst} \times \text{Amount of oxygen atom removal of AgO standard}}{\text{Reducible area of AgO standard} \times \text{weight of catalyst}}$$

$$= \frac{42.29 \times (8.25\times10^{-4}\ \text{mol})}{60.12 \times 0.105\ \text{g}}$$

$$= 5.53 \times 10^{-3}\ \left(\frac{\text{mol}}{\text{g}}\right)$$

Amount of oxygen removed for MnV catalyst $\left(\frac{\text{atom}}{\text{g}}\right)$

= Amount of oxygen removed for MnV catalyst $\left(\frac{\text{mol}}{\text{g}}\right) \times 6.022\times10^{23} \left(\frac{\text{atom}}{\text{mol}}\right)$

$$= 5.53 \times 10^{-3} \frac{\text{mol}}{\text{g}} \times 6.022\times10^{23}\ \left(\frac{\text{atom}}{\text{mol}}\right)$$

APPENDIX C
CALCULATION FOR CATALYTIC PERFORMANCE

The n-pentane conversion and product selectivity were also calculated with the same equations and the calculations are shown in this below.

C.1) Conversion of n-pentane

$$\text{Conversion (\%)} = \frac{\text{Area of n-pentane consumed}}{\text{Area of n-pentane in}}$$

C.2) Selectivity of liquid product

$$\text{Selectivity of MA (\%)} = \frac{\text{Liquid product weight} \times \text{The amount of MA in liquid product}}{\text{MA molecular weight} \times \text{conversion in mole}}$$

$$\text{Selectivity of PA (\%)} = \frac{\text{Liquid product weight} \times \text{The amount of PA in liquid product}}{\text{PA molecular weight} \times \text{Conversion in mole}}$$

C.3) Yield

Yield (%) = Conversion (%) X Selectivity

VITA

Miss Suchanut Pisuttangkul

Birth date : July 4, 1992

Address : 230, Moo. 6, Ban pho Sub-district,
Muang District, Trang, 92000.

Education

High school : Saparachinee trang School

University : The Bachelor's Degree of Chemical Engineering,
Faculty of Engineering, Khon kaen University,
Khon kaen Thailand
Master's Degree of Chemical Engineering at
Department of Chemical Engineering,
Chulalongkorn University, Bangkok Thailand